Background

Recently, the number of patients with colorectal cancer is increasing. Colorectal cancer is the third most common cancer and the fourth most frequent cause of cancer death worldwide [1]. In Japan, colorectal cancer is the third leading cause of cancer-related death.

The prognosis is related to many histopathological and clinical parameters, with the most important prognostic factor affecting survival for patients undergoing curative operation being the presence or absence of regional lymph node involvement [2]. Therefore, it is generally recommended that patients with stage III colorectal cancer, which includes regional lymph node metastases, should undergo adjuvant chemotherapy. However, controversy still exists regarding the necessity of adjuvant chemotherapy for node-negative patients with stage II disease [3]. The QUASAR trial demonstrated that adjuvant chemotherapy with fluorouracil/leucovorin (FU/LV) could improve survival of patients with stage II colorectal cancer, although the absolute improvements were small [4]. Pooled analysis (IMPACT B2) of randomized trials comparing groups with adjuvant chemotherapy receiving FU/LV and those with surgery alone demonstrated that there was no significant difference in event-free and overall survival [5]. Meanwhile, O'Connor et al. reported that no 5-year survival benefit from adjuvant chemotherapy was observed for patients with stage II disease, although a benefit was observed for those with stage III disease [6]. In the present situation, adjuvant chemotherapy is conducted for patients categorized into a high-risk group among those with stage II disease on the basis of various histopathological or clinical parameters such as poorly differentiated histology, lymphovascular invasion, perineural invasion, T4 tumor stage, bowel obstruction or perforation, and an elevated preoperative plasma level of carcinoembryonic antigen (CEA) [7]. These parameters are indicated in some guidelines such as the National Comprehensive Cancer Network (NCCN), European Society for Medical Oncology (ESMO), etc. [8], although they are not based on conclusive evidence.

The immune system discriminates between self and nonself, targeting, for example, cancer cells. However, cancer cells can escape from the immune system and grow, metastasize, and finally cause death. One mechanism of the immune escape by cancer development is the downregulation of human lymphocyte antigen (HLA) class I molecules, which are cancer antigen-presenting molecules for cytotoxic T lymphocytes (CTLs) [9-12]. The immune state is of great importance in the prognosis of cancer patients. Therefore, we focused on the HLA class I expression level in cancer cells to investigate its prognostic value in patients with colorectal cancer. Since most anti-HLA class I antibodies recognize the allele-specific native structure of HLA class I molecules, these antibodies have been unable to react with denatured HLA class I molecules in formalin-fixed paraffin-embedded tissue sections. However, we created a novel monoclonal pan-HLA class I antibody, EMR8-5, suitable for the immunostaining of formalin-fixed tissue specimens [13]. Therefore, we are now able to retrospectively investigate HLA class I expression levels in cancer specimens that were surgically resected and stored for a long time.

In this study, we investigated the prognostic value of HLA class I expression in patients with stage II colorectal cancer.

Methods

Patients

The study was approved by the Clinical Institutional Ethical Review Board of the Medical Institute of Bioregulation, Sapporo Medical University, Japan. We reviewed the clinical pathology archives of 97 consecutive patients with stage II (TNM classification [UICC]) colorectal cancer (61 men and 36 women; age range: 31–83 years) who underwent curative operation, defined as the removal of all of the tumoral masses, the absence of microscopic residual tumors, histology-negative resection margins, and lymphadenectomy extended beyond the involved nodes at the postoperative pathologic examination, at the Sapporo Medical University Hospital, Sapporo, Japan, from February 1994 to January 2005. Written informed consent was obtained from each patient according to the guidelines of the Declaration of Helsinki. Fifty-six patients with poorly differentiated histology or positive lymphovascular invasion had adjuvant chemotherapy. These patients were randomly assigned to receive 5-FU plus daily divided dose cisplatin (5-FU, 320 mg/m^2 daily for 21 days; CDDP, 3.5 mg/m^2 daily for 21 days) followed by oral 5-FU (200 mg/body daily for 2 years) or oral 5-FU therapy (200 mg/body daily for 2 years) exclusively as randomized trial [14]. No patients with rectal cancer had radiotherapy. Patients whose medical reports were incomplete were excluded. The median follow-up time was 54 months. Patients' characteristics were assessed by tumor stage (stage IIA, stage IIB, and stage IIC), age, gender, tumor size, tumor location, histological type, and lymphovascular invasion.

Antibody

The monoclonal anti-pan-HLA class I antibody EMR8-5 was established at our laboratory [13]. This mouse mAb (currently commercially available from Hokudo Co., Ltd., Japan) reacts with extracellular domains of HLA-A*2402, A*0101, A*1101, A*0201, A*0207, B*0702, B*0801, B*1501, B*3501, B*4001, B*4002, B*4006, B*4403, Cw*0102, Cw*0801, Cw*1202, and Cw*1502 [15]

and shows strong reactivity in Western blots and conventional light microscopic analysis of formalin-fixed, paraffin-embedded sections.

Immunohistochemistry

Immunohistochemical staining with the antibody was performed on formalin-fixed, paraffin-embedded tissues after steam heat-induced epitope retrieval. Subsequent incubations with a secondary biotinylated antibody, avidin-conjugated peroxidase complex, and chromogen were carried out on a Ventana NexES (Ventana Medical Systems, Inc., Tucson, AZ) [16]. Slides were then counterstained with hematoxylin, rinsed, dehydrated through graded alcohols into nonaqueous solution, and coverslipped with mounting media. Positive reactivity to EMR8-5 was confirmed by staining of vascular endothelial cells and lymphocytes in sections of tumor specimens [15].

Evaluation of HLA class I expression

The cancer cell membrane immunoreactivity level for HLA class I expressed by EMR8-5 was classified into three categories (positive, dull, and negative). Positive was defined as complete and heterogeneous membrane staining in more than 80% of the tumor cells (Figure 1a). Dull was defined as faint, incomplete, and heterogeneous membrane staining in 20% ~ 80% of the tumor cells (Figure 1b). Negative was defined as membrane staining in less than 20% of the tumor cells (Figure 1c). All specimens were reviewed independently using light microscopy in at least five areas at × 200 magnification by two investigators who were blinded to the clinicopathological data (TT and YI).

Statistical analysis

We investigated the relationships between HLA class I expression levels and the other parameters (age, gender, tumor location, tumor size, depth, histological type, lymphovascular invasion, budding, number of lymph nodes analyzed after surgery (<12), HLA class I expression level, and adjuvant chemotherapy) and clinical outcome (disease-free survival: DFS). Some of these parameters (depth, histological type, lymphovascular invasion, budding, number of lymph nodes analyzed after surgery (<12)) were recommended as potential prognostic factors for curatively resected colorectal cancer by ESMO guidelines [8] or NCCN Guidelines Version 2 (2014). Statistical analysis was performed using SPSS Statistics 17.0. Deviation between the HLA class I expression level and clinicopathological parameters was evaluated with the Pearson χ^2 test. Survival analysis was assessed by the Kaplan-Meier method, and the differences between survival curves were analyzed using the log-rank test. To evaluate the correlations between the survival rate and clinicopathological parameters, univariate and multivariate regression analyses according to the Cox proportional hazards regression model were used. A P value <0.05 was considered to indicate statistical significance.

Results

HLA class I expression level and patient characteristics in patients with stage II colorectal cancer

Immunohistochemical study of HLA class I in cancer cells revealed the following. There were 51 cases (53%) that were positive, which was defined as complete and heterogeneous membrane staining in more than 80% of the tumor cells, as well as 40 (41%) that were dull, which was defined as faint, incomplete, and heterogeneous membrane staining in 20% ~ 80% of the tumor cells, and six (6%) that were negative, which was defined as membrane staining in less than 20% of the tumor cells. In this study, the cases were divided into two groups, those that were "positive" ($n = 51$) and those that were "dull and negative" ($n = 46$). The relationships between HLA class

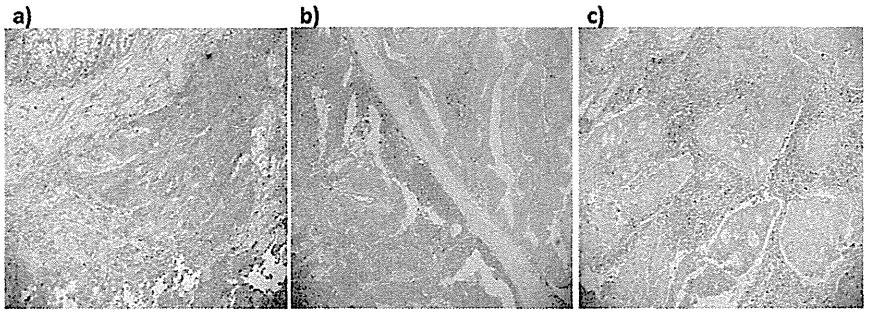

Figure 1 Representative picture of immunostaining with the antibody EMR8-5. The cancer cell membrane immunoreactivity level for HLA class I, which was expressed by EMR8-5, was classified into three categories (positive, dull, and negative). Positive was defined as complete and heterogeneous membrane staining in more than 80% of the tumor cells. Dull was defined as faint, incomplete, and heterogeneous membrane staining in 20% ~ 80% of the tumor cells. Negative was defined as membrane staining in less than 20% of the tumor cells. **(a)** Positive, **(b)** dull, and **(c)** negative.

I expression level and patients' characteristics, i.e., tumor stage (stage IIA, stage IIB, and stage IIC), age, gender, tumor size, tumor location, histological type, and lymphovascular invasion, were assessed. The HLA class I expression level had no significant correlation with other clinicopathological parameters, except for gender (Table 1).

Prognostic factors in patients with stage II colorectal cancer

Univariate analysis related to DFS revealed that the tumor location ($P = 0.01$) and HLA class I expression level ($P = 0.02$) might be significant prognostic factors among age, gender, tumor location, tumor size, depth, histological type, lymphovascular invasion, budding, number of lymph nodes analyzed, HLA class I expression level, and adjuvant chemotherapy. It also suggested that venous invasion might be a prognostic factor ($P = 0.05$). Moreover, multivariate analysis revealed that tumor location, HLA expression level, and venous invasion were significant independent prognostic factors ($P < 0.05$) (Table 2).

HLA class I expression and 5-year DFS

Univariate and multivariate analyses revealed that the HLA class I expression level might be a useful prognostic factor related to DFS. Therefore, survival analysis was conducted using the Kaplan-Meier method. The 5-year DFS rates in the HLA class I positive group and in the dull and negative (dull/negative) group were 89% and 70%, respectively ($P = 0.01$) (Figure 2).

HLA class I expression and adjuvant chemotherapy

Fifty-six stage II colorectal cancer patients with poorly differentiated histology or positive lymphovascular invasion had adjuvant chemotherapy. For patients with this

Table 1 HLA class I expression levels and characteristics of the patients (stage II colorectal cancer)

	Positive ($n = 51$; 53%)	Dull and negative ($n = 46$; 47%)	Total ($n = 97$)	*P* value
Stage				0.54
Stage IIA	46 (90)	42 (91)	88	
Stage IIB	2 (4)	0 (0)	2	
Stage IIC	3 (6)	4 (9)	7	
Age (years)				0.11
Mean ± SD	64 ± 9.7	60 ± 12.3		
Range	42 ~ 80	31 ~ 83		
Gender—no. of patients (%)				0.03
Male	27 (53%)	34 (74%)	61	
Female	24 (47%)	12 (26%)	36	
Diameter of primary tumor (mm)—no. (%)				0.87
≦30	11 (22%)	12 (26%)	23	
31–50	21 (41%)	17 (37%)	38	
≧51	19 (37%)	17 (37%)	36	
Location—no. of patients (%)				0.84
Right	16 (31%)	13 (28%)	29	
Left	15 (30%)	16 (35%)	31	
Rectum	20 (39%)	17 (37%)	37	
Histological type—no. (%)				0.23
Well/mod	48 (94%)	40 (87%)	88	
Por/muc	3 (6%)	6 (13%)	9	
Lymphatic invasion—no. of patients (%)				0.55
Negative	45 (88%)	40 (87%)	85	
Positive	6 (12%)	6 (13%)	12	
Venous invasion—no. of patients (%)				0.33
Negative	44 (86%)	42 (91%)	86	
Positive	7 (14%)	4 (9%)	11	

Table 2 Univariate and multivariate analyses related to disease-free survival in 97 colorectal cancer patients

Variables	Univariate		Multivariate	
	Hazard ratio	*P* value	Hazard ratio	*P* value
Age	0.98 (0.94–1.02)	0.38		
Gender (F)	1.42 (0.50–4.04)	0.51		
Tumor location (colon vs rectum)	4.23 (1.49–12.01)	0.01	4.11 (1.42–11.91)	0.009
Tumor size (≦5 cm)	0.64 (0.24–1.73)	0.38		
Tumor invasion (SI)	0.52 (0.12–2.28)	0.39		
Differentiation (por or muc)	1.50 (0.20–11.35)	0.70		
Lymphatic invasion (ly0, 1 vs ly2, 3)	1.10 (0.25–4.83)	0.90		
Venous invasion (v0, 1 vs v2, 3)	3.10 (1.00–9.56)	0.05	3.85 (1.15–12.92)	0.03
Budding	0.52 (0.19–1.41)	0.20		
Number of lymph nodes analyzed (<12)	1.32 (0.51–3.43)	0.57		
HLA expression level (dull or negative)	3.86 (1.26–11.85)	0.02	5.36 (1.68–17.11)	0.005
Adjuvant chemotherapy (no)	0.82 (0.30–2.22)	0.70		

chemotherapy, the 5-year DFS rates of those with HLA class I positive expression and those with dull/negative expression were compared. The 5-year DFS rates in the HLA class I positive group and in the dull/negative group were 84% and 68%, respectively (Figure 3). The 5-year DFS in patients with HLA dull/negative expression was lower than that of those with HLA positive expression, although there was no significant difference ($P = 0.10$). On the other hand, no patient with HLA class I positive expression without chemotherapy relapsed, whereas 29% of those with HLA dull/negative expression relapsed. For those without adjuvant chemotherapy, there was a significant difference in 5-year DFS between patients with HLA class I positive expression and dull/negative expression ($P = 0.03$) (Figure 4).

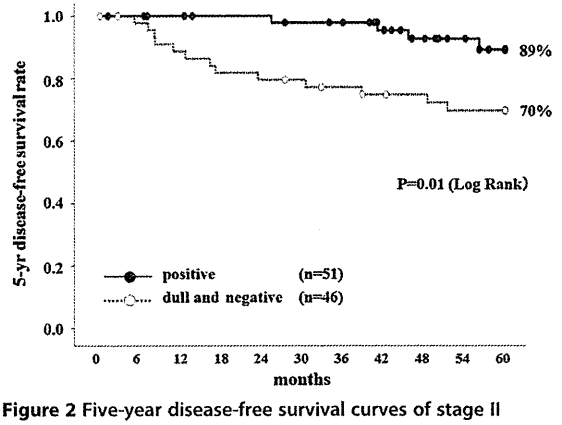

Figure 2 Five-year disease-free survival curves of stage II colorectal cancer patients. The 5-year DFS rates in the HLA class I positive group (*black circle*) and in the dull and negative group (*white circle*) were 89% and 70%, respectively. Patients with HLA class I positive expression had a significantly higher DFS rate than that of those with HLA class I dull and negative expression ($P = 0.01$).

Discussion

Prognostic factors are useful for determination of the therapeutic strategy and follow-up examination after curative operation in cancer treatment. There are various reports of clinical and pathological prognostic factors. However, there are few immunological prognostic factors. The immunological state of the host can influence the prognosis for cancer patients as well as the features of the cancer.

HLA class I molecules have a central role in the anticancer immune system, especially as cancer antigen-presenting molecules for CTLs [13]. CTLs can recognize antigenic peptides presented on the cell surface by HLA

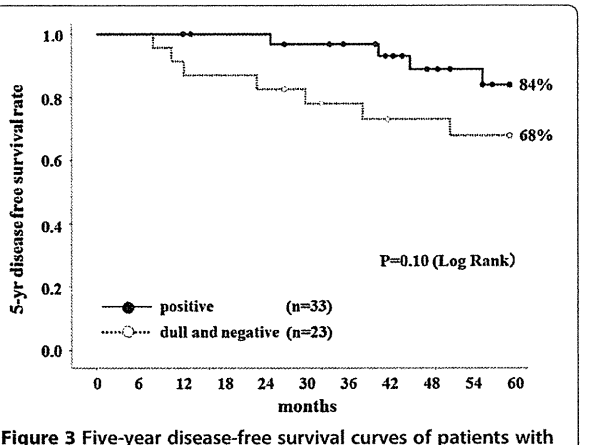

Figure 3 Five-year disease-free survival curves of patients with adjuvant chemotherapy. The 5-year DFS rates of patients with HLA class I positive expression (*black circle*) and with dull and negative expression (*white circle*) were compared. The 5-year DFS in patients with HLA dull and negative expression was decreased more than that of those with HLA positive expression, although there was no significant difference ($P = 0.10$).

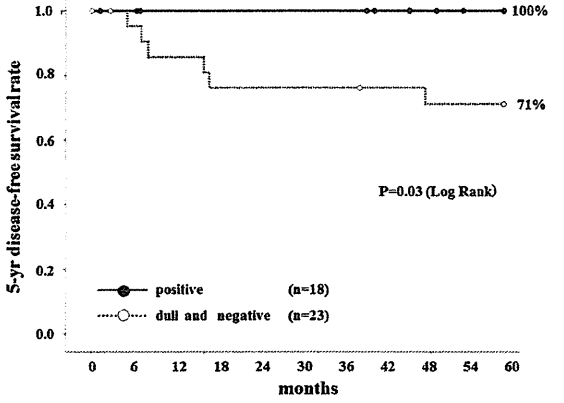

Figure 4 Five-year disease-free survival curves of patients without adjuvant chemotherapy. No patient with HLA class I positive expression (*black circle*) relapsed. Twenty-nine percent of patients with HLA dull and negative expression (*white circle*) relapsed. For patients without adjuvant chemotherapy, there was a significant difference in the 5-year DFS between patients with HLA class I positive expression and those with dull and negative expression ($P = 0.03$).

class I molecules and kill target cells such as cancer cells. However, cancer cells can escape from the immune system by downregulation of HLA class I molecules, secretion of immunosuppressive cytokines, and infiltration of immunosuppressive cells [9-13]. One mechanism of recurrence after curative operation might be immune escape by micrometastatic cancer cells. Therefore, we focused on HLA class I molecules, key molecules in the immune system, to investigate the possibility of new immunological prognostic factors. This investigation was enabled through the use of the novel monoclonal pan-HLA class I antibody EMR8-5 [13], which is suitable for the immunostaining of surgically resected, formalin-fixed tissue specimens stored for a long time.

In this study, we investigated the HLA class I expression level and the prognoses of stage II colorectal cancer patients who underwent curative operation. In patients with stage II cancer, there was a significant difference in 5-year DFS between HLA class I positive patients and dull/negative patients ($P = 0.01$). Patients with HLA class I positive expression had a higher 5-year overall survival (OS) rate than those with HLA class I dull/negative expression, although there was no significant difference ($P = 0.29$) (data not shown). In addition, univariate and multivariate analyses revealed that the HLA class I expression level might be a significant independent prognostic factor. These data suggested that the HLA class I expression level might be a useful prognostic factor, particularly as a predictive factor for relapse, in stage II colorectal cancer. The reason why there was no significant difference in OS for stage II colorectal cancer patients is speculated to be that the beneficial treatments after recurrence might have more influence on OS than the immunological state in the living body such as the HLA class I expression level.

We have also reported that the HLA class I expression level might be a prognostic factor for other cancers such as osteosarcoma, clear cell renal cell carcinoma, and bladder cancer [15-19]. Tsukahara et al. reported that patients with osteosarcoma highly expressing HLA class I had significantly better OS and DFS than those with HLA class I-negative osteosarcoma [15]. Thus, there might be a difference in the impact of the HLA class I expression level on OS or DFS depending on the cancer. Although most reports, including our study, suggested that downregulation of HLA class I expression level was associated with a poor prognosis, Madjd Z et al. reported that total loss of HLA class I was an independent indicator of good prognosis in breast cancer [20]. They considered that the loss of HLA class I might make the tumors more susceptible to natural killer (NK) killing and result in a better prognostic outcome. It is due to the presence of HLA class I allele-specific killer cell inhibitory receptors (KIRs) on the surface of NK cells. Thus, in the absence of HLA class I expression, this KIRs-mediated inhibitory signaling is lost, resulting in the activation of NK cytolytic effector functions [21]. NK cell-mediated cytotoxicity is regulated by a delicate balance between activating and inhibitory signals. So, the prognostic influence brought by the HLA class I expression level might depend on the various cancer immune circumstances.

Surgery alone has relatively favorable results in colorectal cancer patients with stage II disease; hence, any advantage conferred by adjuvant chemotherapy after the curative operation is likely to be small. However, in real life in Japan, approximately 13% of patients with stage II colorectal cancer are found to have recurrence. The seventh edition of the American Joint Committee on Cancer (AJCC) Staging Manual divides stage II into three groups: stage IIA (T3N0), stage IIB (T4aN0), and stage IIC (T4bN0). There is a report that the prognoses for the stage IIB and IIC subgroups are worse than those of some stage III patients [22]. Therefore, stage II patients could be divided into high- and low-risk populations. We should select high-risk stage II patients and give adjuvant chemotherapy to prevent recurrence by micrometastases only to those patients who can obtain a significant benefit from it. The NCCN Guidelines Version 2 (2014) recommended the following risk factors for recurrence: number of lymph nodes analyzed after surgery (<12), poorly differentiated histology, lymphatic/vascular invasion, bowel obstruction, perineural invasion, localized perforation, and close, indeterminate, or positive margins. The ESMO consensus guideline recommended

the following factors: lymph node sampling <12, poorly differentiated tumor, vascular or lymphatic or perineural invasion, T4 stage, and clinical presentation with intestinal occlusion or perforation [8]. In this study, patients with poorly differentiated tumors or moderate and severe lymphovascular invasion were considered to be high-risk stage II patients and underwent adjuvant chemotherapy. We investigated the 5-year DFS in stage II patients with and without adjuvant chemotherapy, respectively. Patients with HLA class I positive expression had a higher DFS rate than those with HLA class I dull/negative expression under both settings. In addition, for low-risk patients without chemotherapy, all patients with HLA class I positive expression did not relapse, although 29% of those with HLA class I dull/negative expression relapsed. These data might make certain of the prognostic value of HLA class I expression for relapse.

Conclusions

The HLA class I expression level might be a very sensitive prognostic factor in colorectal cancer patients with stage II disease.

Abbreviations

DFS: Disease-free survival; CEA: Carcinoembryonic antigen; CTLs: Cytotoxic T lymphocytes; ESMO: European Society for Medical Oncology; NCCN: National Comprehensive Cancer Network; NK: Natural killer; KIRs: Killer cell inhibitory receptors; AJCC: American Joint Committee on Cancer.

Competing interests

The authors declare that they have no competing interests.

Authors' contributions

YI and TT reviewed all specimens stained with the antibody EMR8-5. TM and TF managed the database of colorectal cancer patients. NT performed the statistical analysis. MM and TT carried out the immunohistochemical staining. NS and KH participated in the design and coordination of this study and helped to draft the manuscript. All authors read and approved the final manuscript.

Acknowledgements

Emiri Nakazawa and Kumiko Shimozawa provided EMR8-5.

Author details

[1]Department of Surgery, School of Medicine, Sapporo Medical University, S1, W16, Chuo-ku, Sapporo, Hokkaido 060-0061, Japan. [2]Department of Pathology, School of Medicine, Sapporo Medical University, S1, W16, Chuo-ku, Sapporo, Hokkaido 060-061, Japan.

Received: 31 July 2014 Accepted: 8 January 2015
Published online: 12 February 2015

References

1. Weitz J, Koch M, Debus J, Hohler T, Galle PR, Buchler MW. Colorectal cancer. Lancet. 2005;365:153–65.
2. Onogawa S, Kitadai Y, Tanaka S, Kuwai T, Kimura S, Chayama K. Expression of VEGF-C and VEGF-D at the invasive edge correlates with lymph node metastasis and prognosis of patients with colorectal carcinoma. Cancer Sci. 2004;95:32–9.
3. Wils J. Adjuvant treatment of colon cancer: past, present and future. J Chemotherapy. 2007;19:115–22.
4. Quasar Collaborative Group, Gray R, Barnwell J, McConkey C, Hills RK, Williams NS, et al. Adjuvant chemotherapy versus observation in patients with colorectal cancer: a randomized study. Lancet. 2007;370:2020–9.
5. International Multicentre Pooled Analysis of B2 Colon Cancer Trials (IMPACT B2) Investigators. Efficacy of adjuvant fluorouracil and folinic acid in B2 colon cancer. J Clin Oncol. 1999;17:1356–63.
6. O'Connor ES, Greenblatt DY, LoConte NK, Gangnon RE, Liou JI, Heise CP, et al. Adjuvant chemotherapy for stage II colon cancer with poor prognostic features. J Clin Oncol. 2011;29:3381–8.
7. Wolpin BM, Meyerhardt JA, Mamon HJ, Mayer RJ. Adjuvant treatment of colorectal cancer. CA Cancer J Clin. 2007;57:168–85.
8. Schmoll HJ, Van Cutsem E, Stein A, Valentini V, Glimelius B, Haustermans K, et al. ESMO Consensus Guidelines for management of patients with colon and rectal cancer. A personalized approach to clinical decision making. Ann Oncol. 2012;23:2479–516.
9. Marincola FM, Jaffee EM, Hicklin DJ, Ferrone S. Escape of human solid tumors from T-cell recognition: molecular mechanisms and functional significance. Adv Immunol. 2000;74:181–273.
10. Seliger B, Cabrera T, Garrido F, Ferrone S. HLA class I antigen abnormalities and immune escape by malignant cells. Semin Cancer Biol. 2002;12:3–13.
11. Raffaghello L, Prigione I, Airoldi I, Camoriano M, Morandi F, Bocca P, et al. Mechanisms of immune evasion of human neuroblastoma. Cancer Lett. 2005;228:155–61.
12. Lopez-Albaitero A, Nayak JV, Ogino T, Machandia A, Gooding W, DeLeo AB, et al. Role of antigen-processing machinery in the in vitro resistance of squamous cell carcinoma of the head and neck cells to recognition by CTL. J Immunol. 2006;176:3402–9.
13. Torigoe T, Asanuma H, Nakazawa E, Tamura Y, Hirohashi Y, Yamamoto E, et al. Establishment of a monoclonal anti-pan HLA class I antibody suitable for immunostaining of formalin-fixed tissue: unusually high frequency of down-regulation in breast cancer tissues. Pathol Int. 2012;62:303–8.
14. Hata F, Sasaki K, Hirata K, Yamamitsu S, Shirasaka T. Efficacy of a continuous versus infusion of fluorouracil and daily divided dose cisplatin as adjuvant therapy in resectable colorectal cancer: a prospective randomized trial. Surg Today. 2008;38:623–32.
15. Tsukahara T, Kawaguchi S, Torigoe T, Asanuma H, Nakazawa E, Shimozawa K, et al. Prognostic significance of HLA class I expression in osteosarcoma defined by anti-pan HLA class I monoclonal antibody, EMR8-5. Cancer Sci. 2006;97:1374–80.
16. Le Neel T, Moreau A, Laboisse C, Truchaud A. Comparative evaluation of automated systems in immunohistochemistry. Clin Chim Acta. 1998;278:185–92.
17. Kitamura H, Honma I, Torigoe T, Asanuma H, Sato N, Tsukamoto T. Down-regulation of HLA class I antigen is an independent prognostic factor for clear cell renal cell carcinoma. J Urol. 2007;177:1269–72.
18. Homma I, Kitamura H, Torigoe T, Tanaka T, Sato E, Hirohashi Y, et al. Human leukocyte antigen class I down-regulation in muscle-invasive bladder cancer: its association with clinical characteristics and survival after cystectomy. Cancer Sci. 2009;100:2331–4.
19. Kitamura H, Torigoe T, Honma I, Sato E, Asanuma H, Hirohashi Y, et al. Effects of human leukocyte antigen class I expression of tumor cells on outcome of intravesical instillation of bacillus Calmette-Guerin immunotherapy for bladder cancer. Clin Cancer Res. 2006;12:4641–4.
20. Yabe H, Tsukahara T, Kawaguchi S, Wada T, Torigoe T, Sato N, et al. Prognostic significance of HLA class I expression in Ewing's sarcoma family of tumors. J Surg Oncol. 2011;103:380–5.
21. Madjd Z, Spendlove I, Pinder SE, Ellis IO, Durrant LG. Total loss of MHC class I is an independent indicator of good prognosis in breast cancer. Int J Cancer. 2005;117:248–55.
22. Watson NF, Ramage JM, Madjd Z, Spendlove I, Ellis O, Scholefild JH, et al. Immunosurveillance is active in colorectal cancer as downregulation but not complete loss of MHC class I expression correlates with a poor prognosis. Int J Cancer. 2006;118:6–10.

Immunobiology 220 (2015) 74–82

Contents lists available at ScienceDirect

Immunobiology

journal homepage: www.elsevier.com/locate/imbio

PolyI:C and mouse survivin artificially embedding human 2B peptide induce a CD4+ T cell response to autologous survivin in HLA-A*2402 transgenic mice

Jun Kasamatsu[a,1], Shojiro Takahashi[a,b,1], Masahiro Azuma[a,1,2], Misako Matsumoto[a], Akiko Morii-Sakai[a], Masahiro Imamura[b], Takanori Teshima[b], Akari Takahashi[c], Yoshihiko Hirohashi[c], Toshihiko Torigoe[c], Noriyuki Sato[c], Tsukasa Seya[a,*]

[a] Department of Microbiology and Immunology, Hokkaido University Graduate School of Medicine, Kita-ku, Sapporo, Japan
[b] Department of Hematology, Hokkaido University Graduate School of Medicine, Kita-ku, Sapporo, Japan
[c] Department of Pathology, Sapporo Medical University School of Medicine, Chuoh-ku, Sapporo, Japan

ARTICLE INFO

Article history:
Received 28 March 2014
Received in revised form 4 August 2014
Accepted 6 August 2014
Available online 23 August 2014

Keywords:
Survivin
PolyI:C
CD4 epitope
Peptide vaccine
Th1 response
Interferon-γ
Tumor immunity

ABSTRACT

$CD4^+$ T cell effectors are crucial for establishing antitumor immunity. Dendritic cell maturation by immune adjuvants appears to facilitate subset-specific $CD4^+$ T cell proliferation, but the adjuvant effect for CD4 T on induction of cytotoxic T lymphocytes (CTLs) is largely unknown. Self-antigenic determinants with low avidity are usually CD4 epitopes in mutated proteins with tumor-associated class I-antigens (TAAs). In this study, we made a chimeric version of survivin, a target of human CTLs. The chimeric survivin, where human survivin-2B containing a TAA was embedded in the mouse survivin frame (MmSVN2B), was used to immunize HLA-A-2402/K^b-transgenic (HLA24^b-Tg) mice. Subcutaneous administration of MmSVN2B or xenogeneic human survivin (control HsSNV2B) to HLA24^b-Tg mice failed to induce an immune response without co-administration of an RNA adjuvant polyI:C, which was required for effector induction *in vivo*. Although HLA-A-2402/K^b presented the survivin-2B peptide in C57BL/6 mice, 2B-specific tetramer assays showed that no $CD8^+$ T CTLs specific to survivin-2B proliferated above the detection limit in immunized mice, even with polyI:C treatment. However, the $CD4^+$ T cell response, as monitored by IFN-γ, was significantly increased in mice given polyI:C + MmSVN2B. The Th1 response and antibody production were enhanced in the mice with polyI:C. The CD4 epitope responsible for effector function was not $Hs/MmSNV_{13\text{-}27}$, a nonconserved region between human and mouse survivin, but region 53-67, which was identical between human and mouse survivin. These results suggest that activated, self-reactive $CD4^+$ helper T cells proliferate in MmSVN2B + polyI:C immunization and contribute to Th1 polarization followed by antibody production, but hardly participate in CTL induction.

Introduction

Dendritic cells (DCs) present exogenous antigens (Ags) to cells in the major histocompatibility complex (MHC) class I-restricted Ag-presentation pathway and cause the proliferation of $CD8^+$ T cells specific to the extrinsic Ag. When tumor cells have soluble and insoluble exogenous Ags, MHC class I Ag presentation is mainly transporter associated with antigen processing (TAP)- and proteasome-dependent, suggesting the pathway is partly shared with the pathway for endogenous Ag presentation. The delivery of exogenous Ag by DCs to the pathway for MHC class I-restricted Ag presentation is called cross-presentation (Bevan 1976).

PolyI:C is a double-stranded RNA analog that activates RNA-sensing pattern-recognition receptor pathways (Matsumoto and Seya 2008; Seya and Matsumoto 2009). PolyI:C is an efficient trigger of cross-presentation, and facilitates cross-priming of $CD8^+$ T cells in the presence of Ag. Tumor-associated antigens (TAAs) usually expressed in low levels are thought to need support from pattern-recognition receptor activation to induce TAA-specific cytotoxic T lymphocytes (CTLs) (Seya et al. 2013).

* Corresponding author at: Department of Microbiology and Immunology, Hokkaido University Graduate School of Medicine, Kita 15, Nishi 7, Kita-ku, Sapporo 060-8638, Japan. Tel.: +81 11 706 7866; fax: +81 11 706 7866.
E-mail address: seya-tu@pop.med.hokudai.ac.jp (T. Seya).
[1] These authors equally contributed.
[2] Present address: University of Montreal, 2900 Edouard-Montpetit, Faculty of Medicine/Pavilion Roger Gaudry, Department of Pathology and Cellular Biology, Montreal, QC, H3T 1J4, Canada.

http://dx.doi.org/10.1016/j.imbio.2014.08.017
0171-2985/

Many TAAs have been identified and tested for tolerability to patients and for ability to suppress tumor progression. Peptide vaccine immunotherapy against cancer has been studied clinically (Rosenberg et al. 2004). Survivin (SVN) is a TAA that generates CTLs in cancer patients (Schmitz et al. 2000; Andersen et al. 2001). Human survivin (HsSVN) is a 16.5 kDa cytoplasmic protein that inhibits caspase 3 and 7 in cells stimulated to undergo apoptosis (Altieri 2001). SVN is a member of the inhibitor of apoptosis protein family associated with fetal development. Therefore, except for testis, thymus and placenta, normal tissues express little SVN (Ambrosini et al. 1997; Altieri 2001). SVN is required in early thymocyte development from CD4/CD8-double-negative cells to CD4/CD8-double-positive lymphocytes (Okada et al. 2004). SVN is expressed in a wide variety of malignant cells (Altieri 2001; Fukuda and Pelus 2006). There are several splicing variants including a variant HsSVN2B with a cryptic epitope for MHC class I in humans. An HsSVN2B peptide (AYACNTSTL: 80–88) is an HLA-A*2402-restricted peptide recognized by CD8+ CTLs (Hirohashi et al. 2002). Some cancer cells have higher mRNA levels of the HsSVN splice variant 2B, but whether this splice variant functions in tumorigenesis is unknown (Li 2005).

Several trials have studied the SVN2B peptide in cancer patients (Tsuruma et al. 2008; Honma et al. 2009; Kameshima et al. 2013). Although CTLs specific for SVN were detected in peripheral blood mononuclear cells of most cancer patients, as determined by HLA-A*2402/SVN2B tetramer assays, no substantial therapeutic effect on cancer is seen in most clinical studies. A phase I clinical study found that vaccination with SVN2B peptide combined with IFN-α had significant therapeutic benefits in advanced pancreatic cancer patients, in spite of IFN-mediated side effects. Thus, an IFN-inducing adjuvant, that simultaneously up-regulates Ag-presentation and IFN-inducible genes, might more efficiently contribute to the clinical benefits of SVN for cancer patients.

PolyI:C is an analog of virus double-stranded RNA with IFN-inducing adjuvant properties. To test the effect of polyI:C on survivin-derived CTLs, we used a mouse model expressing human HLA-A24 that presents the SVN2B peptide (Gotoh et al. 2002). Mice have no splice counterpart for HsSVN2B and therefore mouse survivin (MmSVN) lacks the 2B portion of HsSVN, although the mouse ortholog is 84% homologous to HsSVN (Kobayashi et al. 1999). When BALB/c mice are injected intraperitoneally with HsSVN2B + RNA adjuvant, high levels of $CD4^+$ T cells are induced in splenic T cells, as determined by IFN-γ, TNF-α, and IL-2 production, as well as development of lytic MHC class II-restricted T cells and memory (Charalambous et al. 2006).

The N-terminal sequence of HsSVN, which includes amino acids 13–27 (FLKDHRISTFKNWPF), differs from that of MmSVN (YLKNYRIATFKNWPF) (Charalambous et al. 2006). Therefore, high frequencies of self-reactive $CD4^+$ T cells specific for a tumorigenic protein might be elicited in mice with xenogeneic HsSVN. However, self-reactive $CD4^+$ T cells can be induced toward syngeneic or nonmutated CD4 epitopes in cancer patients (Topalian et al. 1996; Osen et al. 2010). To test the possibility that sub-derived self-CD4 epitopes participate in $CD8^+$ CTL proliferation, we made a chimeric survivin protein (MmSVN2B), where the human 2B exon sequence was embedded into MmSVN. We immunized HLA-A-2402/K^b-transgenic ($HLA24^b$-Tg) B6 mice with MmSVN2B. The results indicated that the $CD8^+$ CTL response to a self-tumor Ag (2B peptide) was barely enhanced by treatment of $HLA24^b$-Tg mice with MmSVN2B in the presence of polyI:C. However, $CD4^+$ T cell immune responses to the CD4 epitope of MmSVN2B and HsSVN2B were significantly enhanced in $HLA24^b$-Tg mice with SVN2B proteins + polyI:C. The CD4 epitopes were not the N-terminal $HsSVN_{13-27}$ and $MmSVN_{13-27}$ sequences, but the $Hs/MmSVN_{53-67}$ (DLAQCFFCFKELEGW) sequence, which is identical in HsSVN2B and MmSVN2B and thus a nonmutated CD4 epitope. PolyI:C was required for proliferation of self-reactive $CD4^+$ Th1 cells that recognized the syngeneic epitope. We discuss how RNA adjuvant might induce $CD4^+$ Th1 cells and act in the antitumor immune response.

Materials and methods

Bioinformatics analysis

Ensembl databases (http://asia.ensembl.org/index.html) were used to investigate human and mouse SVN genomic structure. Primate and rodent short interspersed nuclear elements (SINEs) were predicted using the Repeat Masker program (http://www.repeatmasker.org/). Results from databases were confirmed by comparison to previous reports (Mahotka et al. 1999).

Expression analysis

Total RNA was extracted from tissues from C57BL/6 mice and murine cell lines using RNeasy Mini Kits (Qiagen) following the manufacturer's instructions. RT-PCR used High Capacity cDNA Reverse Transcription Kits (Applied Biosystems) according to the manufacturer's instructions. Primer pairs were designed to span separate exons to avoid amplifying other genomic DNA. Primers were 5′-ACTACCGCATCGCCACCT-3′ (forward) and 5′-GCTTGTTGTTGGTCTCCTTTG-3′ (reverse) for detection of the murine SVN gene (MmSVN) and 5′-TGTAACCAACTGGGACGATAT-3′ (forward) and 5′-CTTTTCACGGTTGGCCTTAG-3′ (reverse) for murine *Gapdh*. PCR conditions for mSVN were 94 °C 3 min; 35 cycles of 94 °C 30 s, 65 °C 30 s, 72 °C for 30 s; and 7 min 72 °C. *Gapdh* PCR conditions were 94 °C 3 min; 30 cycles of 94 °C 30 s, 65 °C 30 s, and 72 °C 30 s; and 7 min at 72 °C.

Antigens

The HsSVN2B-coding sequence was amplified using primers 5′-CGGGATCCATGGGTGCCCCGACG-3′ (underline: *Bam*HI site) and 5′-GGAATTCTCAATCCATGGCAGC-3′(underline: *Eco*RI site). To construct the mSVN 2B gene (MmSVN2B), we used two-step PCR to make a chimeric gene of the mSVN gene and the human 2B exon (Fig. 2). In the first PCR, two fragments containing exon 1–2 and exon 3–4 were amplified using primers 5′-CCGCTCGAGATGGGAGCTCCGGCGCT-3′ (underline: *Xho*I site) and 5′-*ACCGTGCCCGGCCCA*ATCGGGTTGTCA-3′ (italics: 5′-end of exon 2B of the HsSVN2B gene) for exon 1 and exon 2 and 5′-*GGGCGGATCACGAGA*GAGGAGCATAGAAAGCA-3′ (italics: 3′-end of exon 2B) and 5′-CGGGATCCTTAGGCAGCCAGCTGCTCAAT-3′ (underline: *Bam*HI site) for exon 3 and exon 4. The exon 2B fragment was amplified using primers 5′-*CGATGACAACCCGATT*GGGCCGGGCACGG-3′ (italics: 3′-end of exon 1 and exon 2 of MmSVN) and 5′-*TTTCTATGCTCCTCTC*TCGTGATCCGCCC-3′ (italics: 5′-end of exon 3 and exon 4 of MmSVN). In the second PCR, the three templates from the first PCR were mixed in equal amounts and amplified using primers 5′-CCGCTCGAGATGGGAGCTCCGGCGCT-3′ (underline: *Xho*I site) and 5′-CGGGATCCTTAGGCAGCCAGCTGCTCAAT-3′ (underline: *Bam*HI site). The pCold vector II (TaKaRa) and SVN fragments were restriction digested and ligated overnight with T4 ligase (Promega) at 4 °C. Ligation mixtures were transformed into competent *Escherichia coli* strain BL21 (DE3) cells. After preculturing for 2 h at 37 °C, cells were cooled on ice. Recombinant protein expression was induced with isopropyl-1-thio-β-D-galactopyranoside at a final concentration of 1 mM and cultured for 24 h at 16 °C. N-His-tagged survivin proteins were purified using a Profinia protein purification system (Biorad). Buffer of

purified SVN proteins was sequentially exchanged with PBS containing 2 M urea. To rule out lipopolysaccharide contamination, we treated survivin proteins with 200 μg/ml of polymixin B (Sigma) for 30 min at 37 °C before use. OVA (ovalbumin) (Sigma) was similarly treated with polymixin B as an Ag.

Mice

C57BL/6 (H-2b) mice were from Clea Japan (Tokyo). HLA24^b-Tg was from SLC Japan (Gotoh et al. 2002). Mice were maintained in the Hokkaido University Animal Facility (Sapporo, Japan) in specific pathogen-free conditions. All experiments used mice that were 8–12 weeks old at the time of first procedure. All mice were used according to the guidelines of the institutional animal care and use committee of Hokkaido University, which approved this study (ID number: 08-0243, "Analysis of immune modulation by toll-like receptors").

Reagents, antibodies and cells

PolyI:C and $OVA_{323-339}$ peptide (ISQAVHAAHAEINEAGR) were from Sigma. $OVA_{257-264}$ peptide (SIINFEKL: SL8), OVA (H2 K^b-SL8), HLA-A*2402 survivin-2B and HIV tetramer were from MBL. SVN2B peptide (AYACNTSTL) and HLA-A*2402/2B peptide-restricted human T cell clones (Idenoue et al. 2005) were kindly provided by Dr. Noriyuki Sato (Department of Pathology, School of Medicine, Sapporo Medical University). Human and murine-specific helper peptides (Charalambous et al. 2006) $MmSVN_{13-27}$ (YLKNYRIATFKNWPF) and Hs SVN_{13-27} (FLKDHRISTFKNWPF) and the common helper peptide Hs/Mm SVN_{53-67} (DLAQCFFCFKELEGW), were synthesized by Biologica Co. Ltd (Nagoya). Peptide purity was >95%. To eliminate lipopolysaccharide contamination, all peptides were treated with 200 μg/ml polymixin B (Sigma) for 30 min at 37 °C before use (Nishiguchi et al. 2001). Anti-CD3ε (145-2C11), anti-CD8α (53-6.7) and anti-IFNγ (XMG1.2) antibodys (Abs) were from BioLegend. Anti-CD4 Ab (L3T4) was from eBiosciences and ViaProbe was from BD Biosciences. Dendritic cells were prepared from spleens of mice as described previously (Azuma et al., 2012).

Antigen-specific T cell expansion in vivo

HLA24^b Tg mice (Gotoh et al. 2002) were subcutaneously immunized with 100 μg of each antigen and 100 μg poly I:C once a week for 4 weeks. After 7 days from the last immunization, spleens were extracted, homogenized and stained with FITC-CD8α and PE-OVA (Azuma et al. 2012) or PE-SVN2B tetramer for detecting antigen-specific CD8$^+$ T cells (Tsuruma et al. 2008). For intracellular cytokine detection, splenocytes were cultured with 100 nM SL8 or survivin 2B peptide for 6 h with 10 μg/ml brefeldin A (Sigma–Aldrich) added in the last 4 h. For intracellular cytokine detection of antigen-specific CD4$^+$ T cells, splenocytes were cultured with 100 nM $OVA_{323-339}$ peptide or SVN helper peptide for 6 h with 10 μg/ml brefeldin A (Sigma–Aldrich) added in the last 5 h. Cells were stained with PE-anti-CD8α/FITC-anti-CD3ε for CD8$^+$ T cells or PE-anti-CD4/FITC-anti-CD3ε for CD4$^+$ T cells. After cell-surface staining, cells were fixed and permeabilized with Cytofix/Cytoperm (BD Biosciences) according to the manufacturer's instruction. Fixed and permeabilized cells were stained with APC-anti-IFN-γ. Stained cells were analyzed with FACSCalibur (BD Biosciences) and FlowJo software (Tree Star) (Azuma et al. 2012).

ELISA

Sera were collected from immunized mice once a week for 4 weeks and 96-well plates were coated with 10 μg/ml OVA, MmSVN2B and HsSVN2B in ELISA/ELISPOT coating buffer (eBioscience) and incubated overnight at 4 °C. ELISA diluent solution (eBioscience) was used for blocking and antibody dilution. PBS with 0.05% Tween 20 was used for washes. Anti-OVA or anti-SVN in sera was assessed by ELISA using antiserum for IgG2a/b and IgG1 diluted 1000-fold and 10,000-fold and incubated for 2 h at room temperature. After washing, isotype IgGs were detected using goat anti-mouse total IgG, IgG1, or IgG2a conjugated to HRP (Southern Biotechnology Associates). After washing, plates were stained with 1XTMB ELISA substrate solution (eBioscience) and reactions stopped with 2 N H_2SO_4 before measuring absorbance.

Statistical analyses

For comparison of two groups, *P*-values were calculated with a Student's *t*-test. For comparison of multiple groups, P-values were calculated with one-way analysis of variance (ANOVA) with Bonferroni's test. Error bars are SD or SEM between samples.

Results

Origin of human SVN exon 2B

The HsSVN gene has four conserved and two cryptic exons (Mahotka et al. 1999). The authentic HsSVN gene encode 142 amino acids in exons 1–4. On the other hand, the HsSVN2B product is 165 amino acids encoded by exons 1, 2, 2B, 3 and 4. Exon 2B is hidden within intron 2, which is spliced into mature HsSVN2B mRNA in-frame between exons 2 and 3 (Mahotka et al. 1999). Exon 2B is followed by the GT-AG role and expressed in many tumor cells and tumor cell lines, suggesting that splicing predominantly occurs in malignantly transformed cells (Mahotka et al. 2002). According to the Ensembl database, HsSVN intron 2 had two Alu sequences (Fig. 1A), and exon 2B resulted from the second Alu. In contrast, the MmSVN gene had four exons separated by three introns with no Alu sequence in intron 2; instead, MmSVN had several SINE sequences characteristic of rodents in intron 2 (Fig. 1A). Although the exon sequences were conserved in human and mouse SVNs, two intron sequences diverged between human and mouse (Fig. 1A). These results suggested that integration of exon 2B was evolutionarily new and formed after an Alu insertion. Although the SVN gene is conserved in yeast and humans, exon 2B was established after the divergence of human and mouse.

We used RT-PCR to investigate transcripts resulting from splicing other exons around exon 2 into the MmSVN mRNA. Results of mRNAs from mouse organs and cell lines are in Fig. 2B. The results suggested that no alternative exons around exon 2 in the MmSVN gene. We detected a ~200 bp product in most organs and cell lines tested (Fig. 2B), but this was not an MmSVN transcript.

Generation of a mmSVN2B construct

A SVN2B peptide derived from the HsSVN2B gene that contained the exon 2B sequence was recognized by CTLs in cancer patients (Hirohashi et al. 2002; Tsuruma et al. 2008; Honma et al. 2009) and a CTL clone was established from patients (Idenoue et al. 2005). We artificially constructed an MmSVN2B with a xenogeneic human exon 2B inserted into the boundary between exon 2 and 3 of SVN (Fig. 2A and B). Prominent amino acid substitutions between MmSVN2B and HsSVN2B were concentrated in the N-terminal region encoded by exon 1 (Fig. 2B), and a CD4 epitope is in this region (Li 2005; Mahotka et al. 2002). In an earlier paper, this $HsSVN_{13-27}$ region, but not $MmSVN_{13-27}$, was an effective CD4 epitope that promoted $HsSVN_{13-27}$-specific CD4$^+$ T cell proliferation

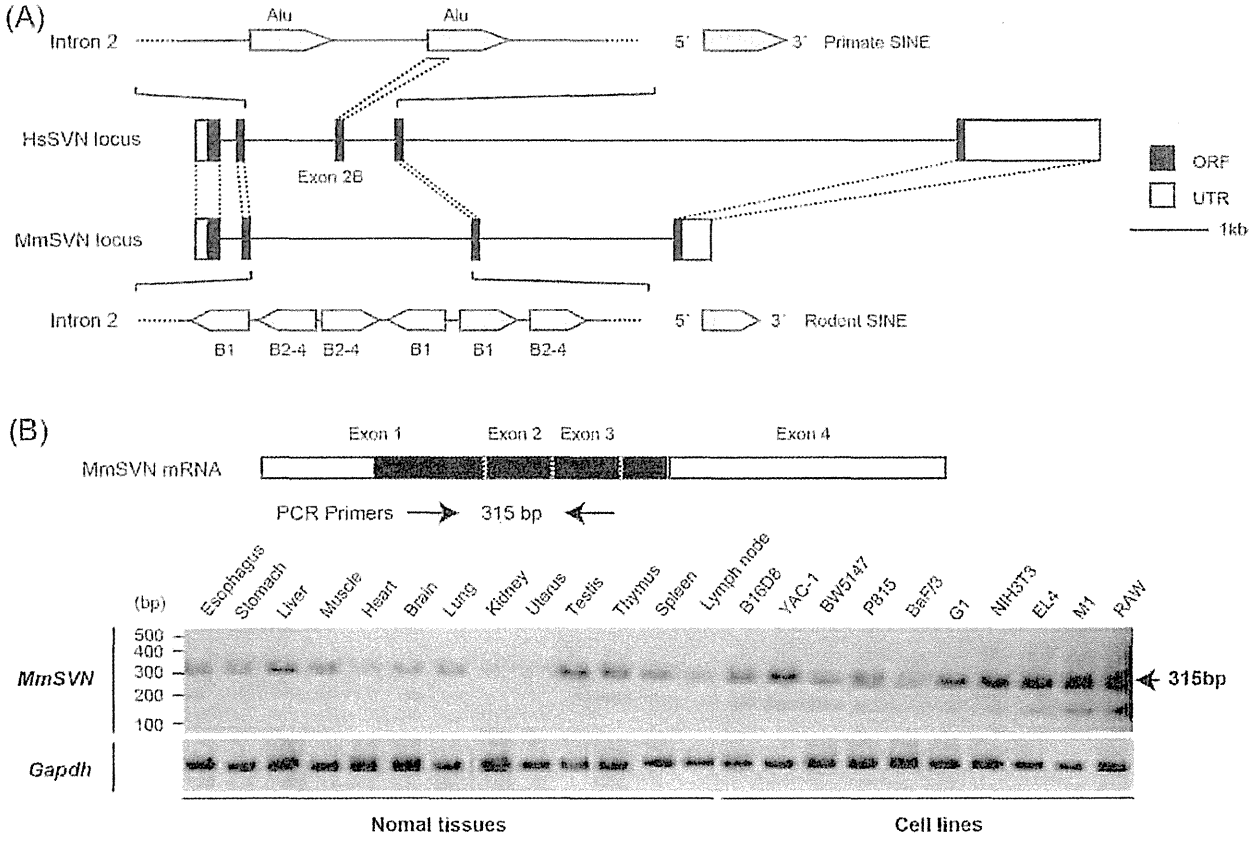

Fig. 1. Genome structure and expression of human and murine SVN gene. (A) Comparison of human and murine survivin gene structure. Survivin gene structures were defined by the Ensembl genome browser. Primate and rodent SINEs were predicted using Repeat Masker program. Filled boxes, coding regions; open boxes, 5′- and 3′-untranslated regions. (B) Structure of murine survivin transcript and RT-PCR analysis of organs and cell lines. Arrows, survivin-detecting PCR primers.

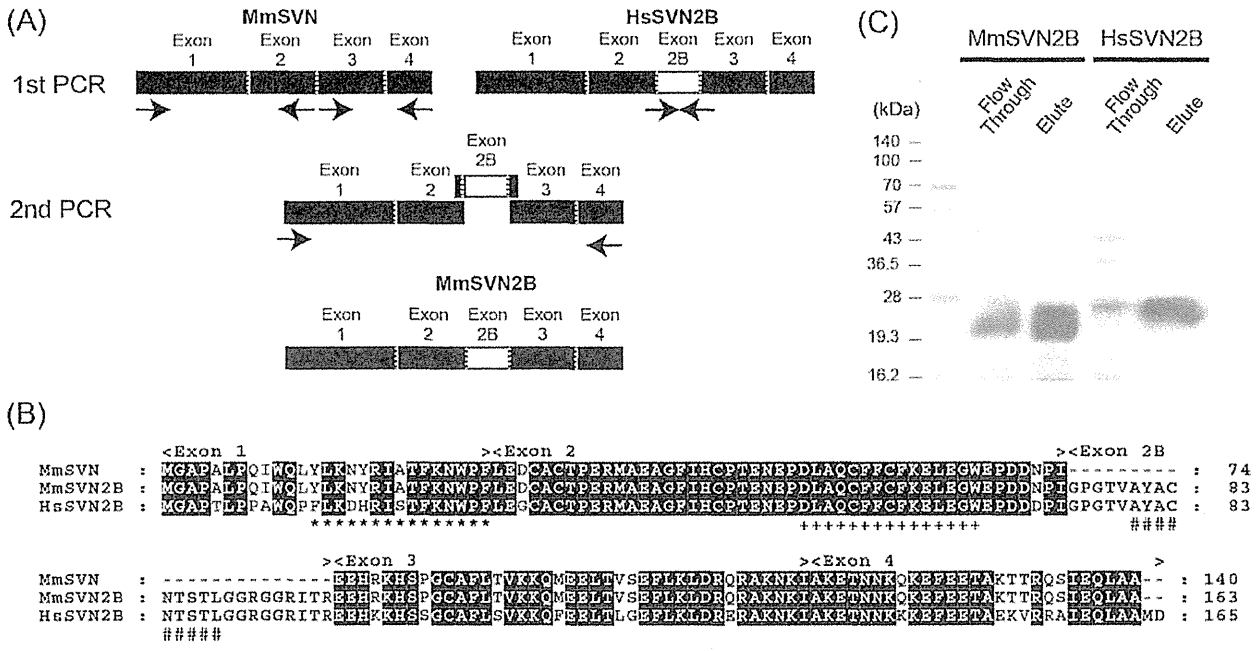

Fig. 2. Structure and purification of chimeric MmSVN2B protein. (A) Strategy for constructing chimeric MmSVN2B protein. Human exon 2B was inserted into MmSVN by PCR. (B) Alignment of murine and human SVN sequences. Black shaded area, residues conserved between human and murine SVN; Hs, human; Mm mouse. *, $MmSVN_{13-27}$/$HsSVN_{13-27}$ peptide; +, Hs/Mm SVN_{53-67} peptide; #, SVN2B peptide. (C) Purification of N-His-tagged MmSVN2B and HsSVN2B proteins. N-His-tagged SVN proteins were purified using a Profinia protein purification system from BL21 (DE3) competent cells. Purified SVN protein buffer was sequentially exchanged to PBS containing 2 M urea.

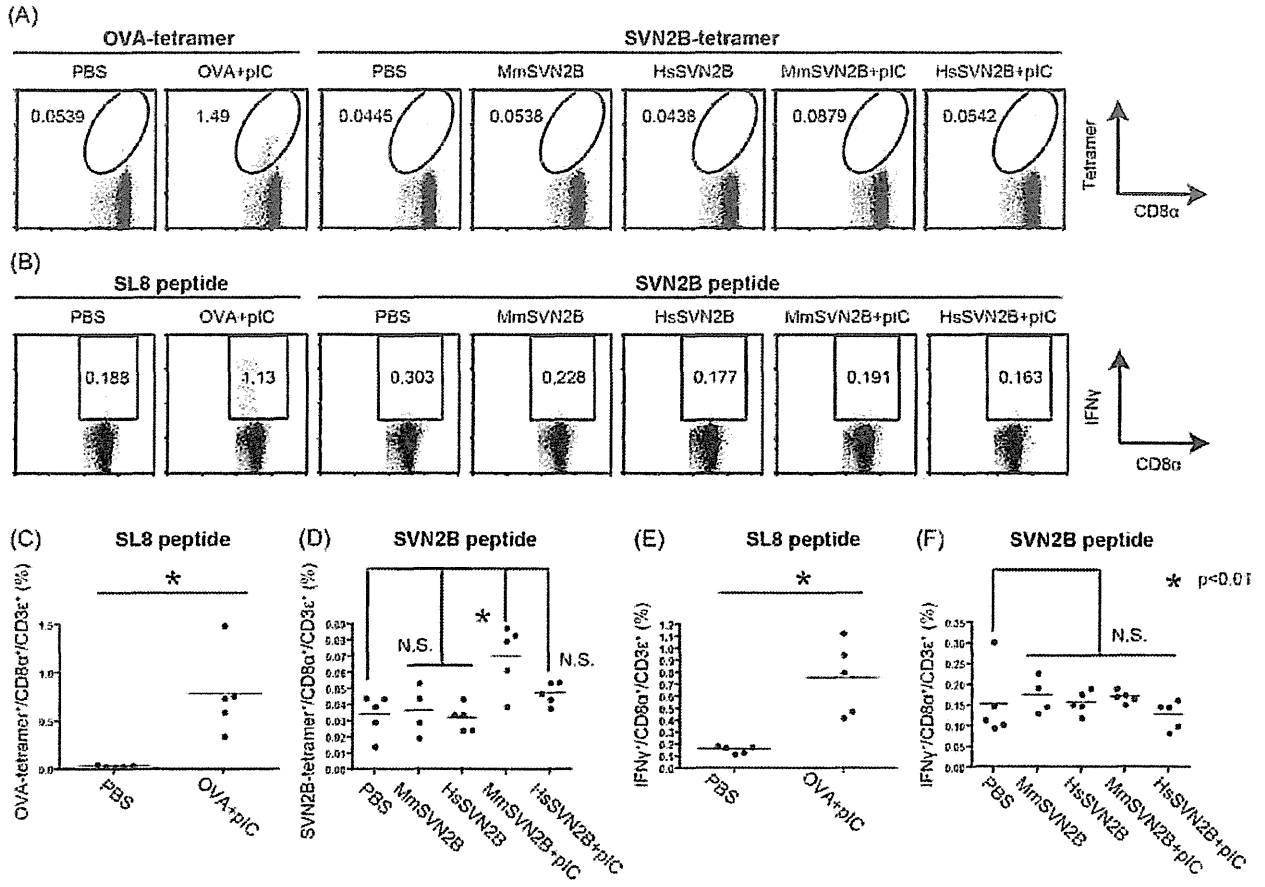

Fig. 3. Expansion of OVA and SVN-specific CD8⁺ T cells. (A) HLA24^b-Tg mice were immunized with 100 μg antigen and 100 μg poly I:C once a week for 4 weeks. After 7 days from the last immunization, spleens were homogenized and stained with FITC-CD8α and PE-OVA or PE-survivin tetramer to detect antigen-specific CD8⁺ T cells. (B) Splenocytes were cultured *in vitro* in the presence of SL8 or SVN2B peptides for 6 h and IFN-γ production was measured by FACS. (C, D) Average percentages of OVA-positive and SVN2B-tetramer positive CD8⁺ T cells shown in (A). (E, F) Average percentages of IFN-γ producing CD8⁺ T cells specifically in response to SL8 or SVN2B peptide in (B). *$p < 0.01$.

(Charalambous et al. 2006). His-tagged MmSVN2B and HsSVN2B proteins were purified and used as Ags (Fig. 2C).

CD4⁺ and CD8⁺ T cells that react to MmSVN2B plus polyI:C

We examined the ability of MmSVN2B to induce IFN-γ and CD8⁺ T cell proliferation by immunizing HLA24^b-Tg mice with MmSVN2B or HsSVN2B with or without polyI:C (Fig. 3). SVN2B-specific CTLs were probed by SVN2B-tetramer (Fig. 3A) and IFN-γ staining (Fig. 3B). SVN2B-specific human CD8⁺ T cells were detected with SVN2B-tetramer (Fig. S1), which enabled us to search for SVN2B-specific CTLs in HLA24^b-Tg mice (Idenoue et al. 2005). Expression of CD40 was up-regulated in CD8α⁺ conventional DCs to a similar extent with MmSVN2B or HsSVN2B (Fig. S2), consistent with a report on CD40 that promotes cross-priming by Ahonen et al. (J Exp Med, 2004). OVA and polyI:C were used as positive controls (Fig. 3A, B left panels), and SL8 (SIINFEKL)-specific CTLs were monitored with OVA tetramer (Azuma et al. 2012). Both OVA-tetramer-positive and IFN-γ-producing CD8⁺ T cells were detected in mice immunized with OVA and polyI:C (Fig. 3C, E). Without polyI:C stimulation, only small number of OVA-tetramer-positive cells were upregulated compared to controls (Azuma et al. 2012; Azuma & Seya unpublished data).

When HLA24^b-Tg mice were immunized with MmSVN2B or HsSVN2B without polyI:C, no significant induction of SVN2B-tetramer-positive (Fig. 3D) or IFN-γ-inducing cells was observed (Fig. 3F). When polyI:C was included, only a small increase in SVN2B-tetramer-positive cells was detected in mice given MmSVN + polyI:C with no significant increase in IFN-γ (Fig. 3F). Mice receiving HsSVN + polyI:C (Fig. 3D) or polyI:C alone (not shown) showed no significant increase in SVN2B-specific CD8⁺ T cells. Consistent with the lack of tetramer-positive CTL induction, MmSVN2B treatment failed to regress MmSVN2B-transfected tumor cells implanted into HLA24^b-Tg mice. In EG7 tumor-bearing mice, administration of polyI:C alone (without Ag) induces tumor-growth retardation due to the contribution of endogenous Ag (Azuma et al. 2012), but in this case with tumor-unloaded mice polyI:C exhibited no tumor-regressing activity (data not shown), possibly due to the lack of Ag.

Next, we determined the amounts of CD4⁺ T cells that reacted with MmSVN2B. The positive control group received OVA Ag and polyI:C (Fig. 4A, B). The negative control group received PBS without Ag and polyI:C, but basal frequencies of IFN-γ-producing CD4⁺ T cells were detected in this group even in the absence of polyI:C or Ag (Fig. 4). When MmSVN2B or HsSVN2B only was used to immunize mice, no significant response was seen in CD4⁺ T cells compared to PBS controls (Fig. 4A, C–E). When polyI:C was included, IFN-γ-producing CD4⁺ T cells restimulated with Hs/MmSVN$_{53-67}$ peptide increased significantly in mice that received MmSVN and HsSVN (Fig. 4C, D). The sequence of MmSVN$_{53-67}$ was identical to the sequence of HsSVN$_{53-67}$ (Fig. 2B). However, we did not detect a significant increase in IFN-γ-producing CD4⁺ T cells in mice

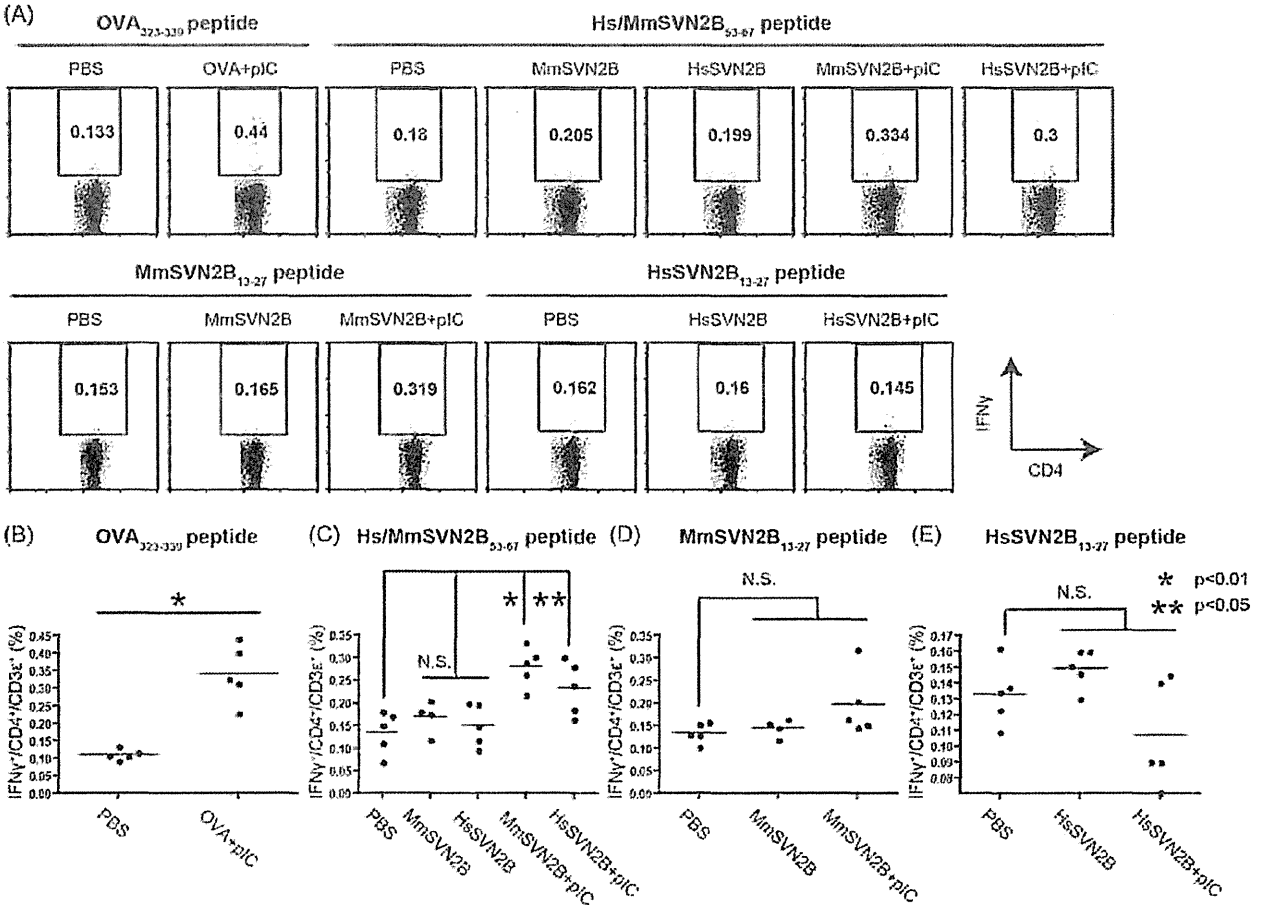

Fig. 4. Expansion of OVA and SVN-specific CD4+ T cells. (A) HLA24b-Tg mice were immunized with 100 μg each antigen and 100 μg poly I:C once a week for 4 weeks. After 7 days from the last immunization, splenocytes were cultured with 100 nM $OVA_{323-339}$ peptide or SVN helper peptide for 6 h, and 10 μg/ml brefeldin A (Sigma–Aldrich) was added in the last 5 h. After cell surface and intracellular staining, IFN-γ production of CD4+ T cells was measured by FACS. Average percentages of IFN-γ-producing CD4+ T cells in response to (B) $OVA_{323-339}$ peptide; (C) Hs/Mm SVN_{53-67} peptide; (D) $MmSVN_{13-27}$ peptide; (E) $HsSVN_{13-27}$ peptide. $^{*}p < 0.01$, $^{**}p < 0.05$.

restimulated with $MmSVN_{13-27}$ or $HsSVN_{13-27}$ peptide (Fig. 4D, E). Differences in these two CD4 epitope sequences are in Fig. 2B.

Ab production by immunization with MmSVN2B with polyI:C

Activation of Th1 cells is essential for B cell antibody class switching. Therefore, we examined production of SVN-specific Ab in Tg mice that did or did not receive polyI:C. Serum was collected from HLA24b-Tg mice immunized with different Ags and polyI:C. OVA and polyI:C were the positive control and resulted in a significant increase in OVA-specific IgG1, IgG2a and IgG2b by ELISA (Fig. 5 left panels). When HLA24b-Tg mice were immunized with MmSVN2B or HsSVN2B without polyI:C, no significant production of any isotypes was observed (Fig. 5 center and right panels). When polyI:C was included, MmSVN2B or HsSVN2B-specific isotypes increased significantly.

Discussion

We demonstrated that HLA24b-Tg mice induced $Hs/MmSVN_{53-67}$-specific CD4+ T cells and SVN-specific Ab followed by Th1 cell activation in response to injection of polyI:C and MmSVN2B protein. This result was partly inconsistent with a previous report (Charalambous et al. 2006) using Balb/c mice and HsSVN conjugated to Dec205 mAb. That is, our study with C57BL/6 mice and MmSVN2B did not detect significant increases in $MmSVN_{13-27}$-specific CD4+ T cells after subcutaneous injection of MmSVN2B with polyI:C. Thus, the xenogeneic differences in sequence between HsSVN and MmSVN did not always contribute to generating effective CD4+ T cells specific for a tumorigenic protein in C57BL/6 mice. The haplotype of the MHC class II proteins between Balb/c (having H-2d) and C57BL/6 mice (having H-2b) and Dec205 mAb conjugation (Charalambous et al. 2006) might be the reason for these different results. However, no CD8+ CTLs against the 2B peptide were detected even when using a specific tetramer for detection of CD8+ CTLs (Fig. S1). Hence, polyI:C was required for proliferation of self-reactive CD4+ Th1 cells that recognized the syngeneic epitope without proliferation of SVN2B peptide-specific CTLs.

OVA were used as positive controls (Fig. 3A, B left panels), and SL8 (SIINFEKL)-specific CTLs were monitored with OVA tetramer (Azuma et al. 2012). Here, T cell activation by polyI:C + MmSVN2B is a focus in this study. However, there is a lot-to-lot difference of T cell-activating activity in polyI:C + OVA as in our present and previous studies (Azuma et al. 2012). This difference of T cell activation may be attributable to the fact that polyI:C consists of a variety of length of polyI chains and polyC chains with a lot-to-lot heterogeneity. In addition, the amounts of Ags in Azuma's experiment are higher than those in the present experiment (Azuma et al. 2012). CD40 stimulation by specific Ab results in high enhancement of cross-priming of CD8 T cells (Charalambous et al. 2006) and CD40 was up-regulated in CD8α+ DCs by polyI:C treatment, but the CD40

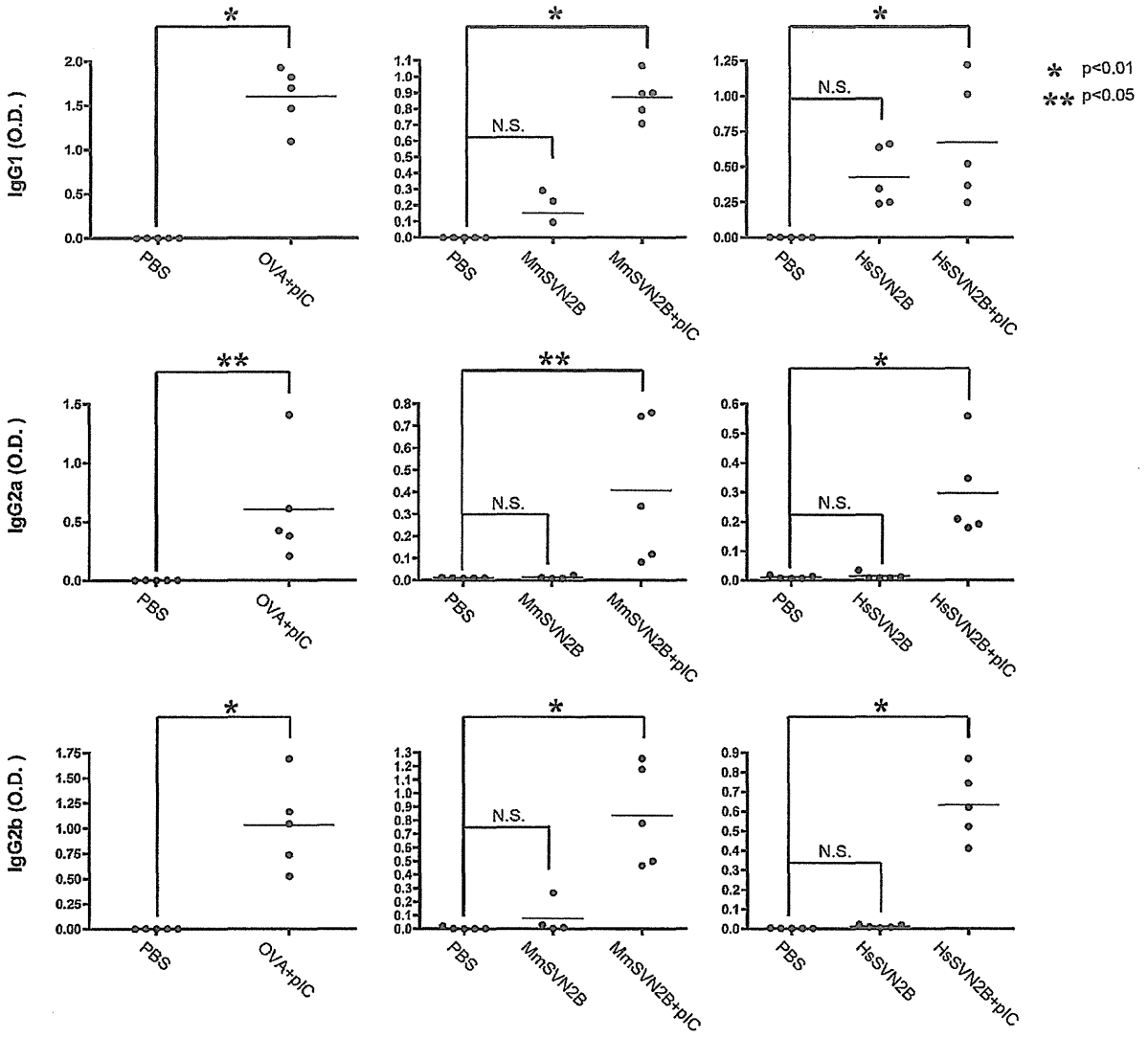

Fig. 5. Production of OVA and SVN-specific antibodies. Sera were collected from immunized mice at once a week for 4 weeks. Anti-OVA or anti-SVN in sera was assessed by ELISA using antiserum for IgG2a/b and IgG1. $^{*}p < 0.01$, $^{**}p < 0.05$.

levels were also variable depending upon the polyI:C lots. Development of a synthesizing method for defined length of RNA duplex will settle the issue.

Two points are noted. First, polyI:C, an RNA adjuvant, induces $CD4^+$ T cells in addition to the reported cases of $CD8^+$ T cells. The factors that participate in polyI:C-mediated CD4+ T cell proliferation and the kind of $CD4^+$ T subsets that are predominantly induced by polyI:C remain unknown. PolyI:C is primarily a potential activator of the IFN-inducing pathways RIG-I/MDA5 and TLR3 (Matsumoto & Seya 2008). These pathways allow host immune cells to produce type I/III IFNs and cytokines and are soluble effectors against cancer. TLR3 preferentially induces cross-presentation in $CD8\alpha^+$ DC in response to dsRNA including polyI:C (Schulz et al., 2005; Azuma et al. 2012) and causes proliferation of $CD8^+$ T cells including cells that respond to TAAs *via* cross-priming (Azuma et al. 2012). $CD4^+$ T cells that are likely evoked by polyI:C stimulation function in antitumor immunity since their helper function is usually suppressed in tumor-bearing mice and can be relieved by innate immune response (Lee et al. 2013). Stimulation with polyI:C + SVN Ag might change a tumor-derived suppressive environment to an environment suitable for primary activation and maintenance of Ag-specific cytotoxic $CD8^+$ T cell responses (Ridge et al. 1998; Janssen et al. 2003).

According to a recent report, however, adoptively transferred $CD4^+$ T cells induce tumor rejection independently of $CD8^+$ T cells (Corthay et al. 2005; Perez-Diez et al. 2007). This rejection is apparently based on cytokines released from $CD4^+$ T cells (Corthay et al. 2005) and on interaction with $CD4^+$ T cells and other immune cells such as macrophages (Mfs) and natural killer (NK) cells (Perez-Diez et al. 2007). DCs stimulated with polyI:C also result in NK cell activation after DC-NK cell-to-cell contact (Akazawa et al. 2007). Mfs in tumors might be a direct target of dsRNA, which converts tumor-supporting Mfs into tumoricidal Mfs (Shime et al. 2012). IL-12p40 is preferentially produced *via* the TICAM-1/Batf3 pathway in response to dsRNA (Azuma et al. 2013). Thus, a variety of cellular effectors can be triggered as antitumor agents by administration of dsRNA with TAA peptides or proteins. We found that $CD4^+$ T cells with Th1 properties were effectors induced by polyI:C possibly acting as an antitumor agent in SVN-responding tumor cells. Although epitope sequence and hydrophobicity might affect Th1 polarization in mice, $CD4^+$ T effectors are successfully induced in tumor-bearing or tumor-implanted mice by stimulation with MmSVN2B + polyI:C.

Hence, *in vivo* administration of an RNA adjuvant with Ag proteins induce $CD4^+$ helper T cells secondary to class II presentation in DCs, together with induction of type I IFNs and cytokines. $CD4^+$ T cells also facilitate Ab production caused by stimulation of B cell development (Mak et al. 2003).

Notably, this is a specific feature of RNA adjuvants, since TLR2 agonist Pam2 lipopeptides such as Pam2CSK4 and MALP2s induce antitumor CTLs with sufficient potential (Chua et al. 2014) but fail to induce DC-mediated antitumor NK cell activation (Yamazaki et al. 2011; Sawahata et al. 2011). $CD4^+$ T cells with regulatory modes such as Tregs and Tr-1 cells and IL-10 were induced by Pam2 peptide in the presence of Ag (Yamazaki et al. 2011). Nevertheless, robust proliferation of antitumor CTL is induced by Pam2 lipopeptides (Chua et al. 2014). Thus, the mode of $CD8^+$ T cell proliferation is differentially modulated between TLR2 and TLR3/MDA5 agonists.

The other point is how self-Ag-reactive $CD4^+$ T cells that act as Th1 effectors in SVN-based immunotherapy are generated. Proliferation of self-reactive T cells is prevented in normal mice, so the levels of self-reactive T cells are usually lower than the detection limit of assays (Gebe et al. 2003). Self-reactive $CD4^+$ T cells might be positively regulated by polyI:C in the presence of protein antigen, since mice, when exposed to DNA/RNA, harbor autoimmune diseases against the protein (Mills 2011). However, even with Ag proteins, polyI:C induced minimal cross-priming of $CD8^+$ T cells in our setting, as with previous reports (Charalambous et al. 2006). In this and other studies, both syngeneic and xenogeneic CD4 epitopes prime $CD4^+$ T cells, stimulating Ab production and Th1 polarization with antitumor activity, but with little association with CTL induction (Charalambous et al. 2006). Our SVN results suggested that self-responsive CD4 epitopes that are identical in sequence in human and mouse SVN have a conserved function as a Th1 skewer, albeit modest, in mice by stimulating DCs and Mfs to prime T and B cells. In this context, however, a question remains to be settled about why the insertion of the 2B sequence in MmSVN caused induction of auto-reactive $CD4^+$ T cells secondary to the class II presentation of the common SVN sequence (53-67) rather than the reported uncommon 13–27 region.

Generally, the presence of Tregs and regulatory cytokines such as IL-10 usually suppresses the function of self-reactive $CD4^+$ T effectors, so an autoimmune response cannot be detected (Danke et al. 2004; Quezada et al. 2010). In tumor-bearing mice, polyI:C releases the restriction of T cell autoreactivity by Tregs to enhance $CD4^+$ T function in a tumor microenvironment. Although the level of Treg cells increases in MALP2s-stimulated tumor-bearing mice (Yamazaki et al. 2011), the amount of Treg cells is not affected by polyI:C injection (Chua et al. 2014). Signs of autoimmune diseases have not yet been observed in mice that received intermittent administration of polyI:C under our conditions. Further studies on the function of regulatory factors in tumor-bearing mice after treatment with various adjuvants are needed to determine the balance between $CD4^+$ T effector functions and regulatory factors including Tregs (Quezada et al. 2010; Corthay et al. 2005).

It has been reported that treatment of murine glioma with DCs loading MmSVN long overlapping peptide covering CD4 and CD8 epitopes (DC therapy) conferred good prognosis on tumor-bearing mice (Ciesielski et al., 2008). In previous trials on peptide vaccine therapy, SVN2B peptide + IFN-α resulted in clinical improvements and enhanced immunological responses of patients (Kameshima et al. 2013). Treatment with SVN2B peptide alone did not result in good prognosis or effective tumor regression in late stage patients with cancer, however (Tsuruma et al. 2008; Honma et al. 2009). These results suggest that both killer and helper T cells are required for *in vivo* induction of tumor regression, as previously suggested (Perez-Diez et al. 2007). NK cells, Mfs, and soluble and angiogenetic factors might be involved in tumor rejection (Shime et al. 2012; Müller-Hermelink et al., 2008; Coussens and Werb 2002) in addition to Ag + polyI:C. According to the study with Ag and polyI:C, a protein or long peptide Ag containing CD4 epitopes, adjuvant RNA and additional factors that disable immunoregulatory factors, are required to effectively induce TAA-specific killer and helper T cell proliferation and subsequent tumoricidal activity in future studies (Casares et al. 2001). Ag peptides should be designed to present both class I and class II peptides on DCs to facilitate proliferation of $CD4^+$ T cells and Ab production. Methods for inducing potential $CD8^+$ CTLs against tumors still need to be considered.

Competing interests

The authors have declared that no competing interest exists.

Acknowledgements

We are grateful to members in our laboratories. JK is a Research Fellow of the Japan Society for the Promotion of Science. This work was supported in part by Grants-in-Aid from the Ministry of Education, Science, and Culture and the Ministry of Health, Labor, and Welfare of Japan, and by a MEXT Grant-in-Project 'the Carcinogenic Spiral', 'the National Cancer Center Research and Development Fund (23-A-44)'. Financial support by the Takeda Science Foundation, the Yasuda Cancer Research Foundation and the Ono Foundation are gratefully acknowledged.

Appendix A. Supplementary data

Supplementary data associated with this article can be found, in the online version, at http://dx.doi.org/10.1016/j.imbio.2014.08.017.

References

Ahonen, C.L., Doxsee, C.L., McGurran, S.M., Riter, T.R., Wade, W.F., Barth, R.J., Vasilakos, J.P., Noelle, R.J., Kedl, R.M., 2004. Combined TLR and CD40 triggering induces potent CD8+ T cell expansion with variable dependence on type I IFN. J. Exp. Med. 199, 775–784.

Altieri, D.C., 2001. The molecular basis and potential role of survivin in cancer diagnosis and therapy. Trends Mol. Med. 7, 542–547.

Akazawa, T., Ebihara, T., Okuno, M., Okuda, Y., Shingai, M., Tsujimura, K., Takahashi, T., Ikawa, M., Okabe, M., Inoue, N., Okamoto-Tanaka, M., Ishizaki, H., Miyoshi, J., Matsumoto, M., Seya, T., 2007. Antitumor NK activation induced by the Toll-like receptor 3-TICAM-1 (TRIF) pathway in myeloid dendritic cells. Proc. Natl. Acad. Sci. U. S. A. 104, 252–257.

Ambrosini, G., Adida, C., Altieri, D.C., 1997. A novel anti-apoptosis gene, survivin, expressed in cancer and lymphoma. Nat. Med. 3, 917–921.

Andersen, M.H., Pedersen, L.O., Becker, J.C., Straten, P.T., 2001. Identification of a cytotoxic T lymphocyte response to the apoptosis inhibitor protein survivin in cancer patients. Cancer Res. 61, 869–872.

Azuma, M., Ebihara, T., Oshiumi, H., Matsumoto, M., Seya, T., 2012. Cross-priming for antitumor CTL induced by soluble Ag + polyI:C depends on the TICAM-1 pathway in mouse CD11c(+)/CD8α(+) dendritic cells. Oncoimmunology 1, 581–592.

Azuma, M., Matsumoto, M., Seya, T., 2013. PolyI:C-derived dendritic cell maturation and cellular effectors depend on TICAM-1-Batf3 axis in mice. Proc. Jpn. Cancer Assoc. 72, 126.

Bevan, M.J., 1976. Cross-priming for a secondary cytotoxic response to minor H antigens with H-2 congenic cells which do not cross-react in the cytotoxic assay. J. Exp. Med. 143, 1283–1288.

Casares, N., Lasarte, J.J., de Cerio, A.L., Sarobe, P., Ruiz, M., Melero, I., Prieto, J., Borrás-Cuesta, F., 2001. Immunization with a tumor-associated CTL epitope plus a tumor-related or unrelated Th1 helper peptide elicits protective CTL immunity. Eur. J. Immunol. 31, 1780–1789.

Charalambous, A., Oks, M., Nchinda, G., Yamazaki, S., Steinman, R.M., 2006. Dendritic cell targeting of survivin protein in a xenogeneic form elicits strong CD4+ T cell immunity to mouse survivin. J. Immunol. 177, 8410–8421, 44.

Chua, B.Y., Olson, M.R., Bedoui, S., Sekiya, T., Wong, C.Y., Turner, S.J., Jackson, D.C., 2014. The use of a TLR2 agonist-based adjuvant for enhancing effector and memory CD8 T-cell responses. Immunol. Cell Biol., http://dx.doi.org/10.1038/icb.2013.102.

Ciesielski, M.J., Kozbor, D., Castanaro, C.A., Barone, T.A., Fenstermaker, R.A., 2008. Therapeutic effect of a T helper cell supported CTL response induced by a survivin peptide vaccine against murine cerebral glioma. Cancer Immunol. Immunother. 57, 1827–1835.

Corthay, A., Skovseth, D.K., Lundin, K.U., Rosjo, E., Omholt, H., Hofgaad, P.O., Haraldsen, G., Bogen, B., 2005. Primary antitumor immune response mediated by CD4+ T cells. Immunity 22, 371–383.

Coussens, L.M., Werb, Z., 2002. Inflammation and cancer. Nature 420, 860–867.

Danke, N.A., Koelle, D.M., Yee, C., Beheray, S., Kwok, W.W., 2004. Autoreactive T cells in healthy individuals. J. Immunol. 172, 5967–6572.

Fukuda, S., Pelus, L.M., 2006. Survivin, a cancer target with an emerging role in normal adult tissues. Mol. Cancer Ther. 5, 1087–1098.

Gebe, J.A., Falk, B.A., Rock, K.A., Kochik, S.A., Heninger, A.K., Reijonen, H., Kwok, W.W., Nepom, G.T., 2003. Low-avidity recognition by CD4+ T cells directed to self-antigens. Eur. J. Immunol. 33, 1409–1417.

Gotoh, M., Takasu, H., Harada, K., Yamaoka, T., 2002. Development of HLA-A2402/K^b transgenic mice. Int. J. Cancer 100, 565–570.

Hirohashi, Y., Torigoe, T., Maeda, A., Nabeta, Y., Kamiguchi, K., Sato, T., Yoda, J., Ikeda, H., Hirata, K., Yamanaka, N., Sato, N., 2002. An HLA-A24-restricted cytotoxic T lymphocyte epitope of a tumor-associated protein, survivin. Clin. Cancer Res. 8, 1731–1739.

Honma, I., Kitamura, H., Torigoe, T., Takahashi, A., Tanaka, T., Sato, E., Hirohashi, Y., Masumori, N., Tsukamoto, T., Sato, N., 2009. Phase I clinical study of anti-apoptosis protein survivin-derived peptide vaccination for patients with advanced or recurrent urothelial cancer. Cancer Immunol. Immunother. 58, 1801–1807.

Idenoue, S., Hirohashi, Y., Torigoe, T., Sato, Y., Tamura, Y., Hariu, H., Yamamoto, M., Kurotaki, T., Tsuruma, T., Asanuma, H., Kanaseki, T., Ikeda, H., Kashiwagi, K., Okazaki, M., Sasaki, K., Sato, T., Ohmura, T., Hata, F., Yamaguchi, K., Hirata, K., Sato, N., 2005. A potent immunogenic general cancer vaccine that targets survivin, an inhibitor of apoptosis proteins. Clin. Cancer Res. 11, 1474–1482.

Janssen, E.M., Lemmens, E.E., Wolfe, T., Christen, U., von Herrath, M.G., et al., 2003. CD4+ T cells are required for secondary expansion and memory in CD8+ T lymphocytes. Nature 421, 852–856.

Kameshima, H., Tsuruma, T., Kutomi, G., Shima, H., Iwayama, Y., Kimura, Y., Imamura, M., Torigoe, T., Takahashi, A., Hirohashi, Y., Tamura, Y., Tsukahara, T., Kanaseki, T., Sato, N., Hirata, K., 2013. Immunotherapeutic benefit of α-interferon (IFNα) in survivin2B-derived peptide vaccination for advanced pancreatic cancer patients. Cancer Sci. 104, 124–129.

Kobayashi, K., Hatano, M., Otaki, M., Ogasawara, T., Tokuhisa, T., 1999. Expression of a murine homologue of the inhibitor of apoptosis protein is related to cell proliferation. Proc. Natl. Acad. Sci. U. S. A. 96, 1457–1462.

Lee, M.K.4th, Xu, S., Fitzpatrick, E.H., Sharma, A., Graves, H.L., Czerniecki, B.J., 2013. Inhibition of CD4+CD25+ regulatory T cell function and conversion into Th1-like effectors by a Toll-like receptor-activated dendritic cell vaccine. PLOS ONE 8, e74698.

Li, F., 2005. Role of survivin and its splice variants in tumorigenesis. Br. J. Cancer 92, 212–216.

Mahotka, C., Wenzel, M., Springer, E., Gabbert, H.E., Gerharz, C.D., 1999. Survivin-deltaEx3 and survivin-2B: two novel splice variants of the apoptosis inhibitor survivin with different antiapoptotic properties. Cancer Res. 59, 6097–6102.

Mahotka, C., Liebmann, J., Wenzel, M., Suschek, C.V., Schmitt, M., Gabbert, H.E., Gerharz, C.D., 2002. Differential subcellular localization of functionally divergent surviving splice variants. Cell Death Differ. 9, 1334–1342.

Mak, T.W., Shahinian, A., Yoshinaga, S.K., Wakeham, A., Boucher, L.M., Pintilie, M., Duncan, G., Gajewska, B.U., Gronski, M., Eriksson, U., Odermatt, B., Ho, A., Bouchard, D., Whorisky, J.S., Jordana, M., Ohashi, P.S., Pawson, T., Bladt, F., Tafuri, A., 2003. Costimulation through the inducible costimulator ligand is essential for both T helper and B cell functions in T cell-dependent B cell responses. Nat. Immunol. 4, 765–772.

Matsumoto, M., Seya, T., 2008. TLR3: interferon induction by double-stranded RNA including poly(I:C). Adv. Drug Deliv. Rev. 60, 805–812.

Mills, K.H., 2011. TLR-dependent T cell activation in autoimmunity. Nat. Rev. Immunol. 11, 807–822.

Müller-Hermelink, N., Braumüller, H., Pichler, B., Wieder, T., Mailhammer, R., Schaak, K., Ghoreschi, K., Yazdi, A., Haubner, R., Sander, C.A., Mocikat, R., Schwaiger, M., Förster, I., Huss, R., Weber, W.A., Kneilling, M., Röcken, M., 2008. TNFR1 signaling and IFN-gamma signaling determine whether T cells induce tumor dormancy or promote multistage carcinogenesis. Cancer Cell 13, 507–518.

Nishiguchi, M., Matsumoto, M., Takao, T., Hoshino, M., Shimonishi, Y., Tsuji, S., Begum, N.A., Takeuchi, O., Akira, S., Toyoshima, K., Seya, T., 2001. Mycoplasma *fermentans* lipoprotein M161Ag-induced cell activation is mediated by Toll-like receptor 2: role of N-terminal hydrophobic portion in its multiple functions. J. Immunol. 166, 2610–2616.

Okada, H., Bakal, C., Shahinian, A., Elia, A., Wakeham, A., Suh, W.K., Duncan, G.S., Ciofani, M., Rottapel, R., Zuniga-Pflucker, J.C., Mak, T.W., 2004. Survivin loss in thymocytes triggers p53-mediated growth arrest and p53-independent cell death. J. Exp. Med. 199, 399–410.

Osen, W., Soltek, S., Song, M., Leuchs, B., Steitz, J., Tüting, T., Eichmüller, S.B., Nguyen, X.D., Schadendorf, D., Paschen, A., 2010. Screening of human tumor antigens for CD4T cell epitopes by combination of HLA-transgenic mice, recombinant adenovirus and antigen peptide libraries. PLOS ONE 5, e14137.

Perez-Diez, A., Joncker, N.T., Choi, K., Chan, W.F., Anderson, C.C., Lantz, O., Matzinger, P., 2007. CD4 cells can be more efficient at tumor rejection than CD8 cells. Blood 109, 5346–5354.

Quezada, S.A., Simpson, T.R., Peggs, K.S., Merghoub, T., Vider, J., Fan, X., Blasberg, R., Yagita, H., Muranski, P., Antony, P.A., Restifo, N.P., Allison, J.P., 2010. Tumor-reactive CD4(+) T cells develop cytotoxic activity and eradicate large established melanoma after transfer into lymphopenic hosts. J. Exp. Med. 207, 637–650.

Ridge, J.P., Di Rosa, F., Matzinger, P., 1998. A conditioned dendritic cell can be a temporal bridge between a CD4+ T-helper and a T-killer cell. Nature 393, 474–478.

Rosenberg, S.A., Yang, J.C., Restifo, N.P., 2004. Cancer immunotherapy: moving beyond current vaccines. Nat. Med. 10, 909–915.

Sawahata, R., Shime, H., Yamazaki, S., Inoue, N., Akazawa, T., Fujimoto, Y., Fukase, K., Matsumoto, M., Seya, T., 2011. Failure of mycoplasma lipoprotein MALP-2 to induce NK cell activation through dendritic cell TLR2. Microbes Infect. 13, 350–358.

Schmitz, M., Diestelkoetter, P., Weigle, B., Schmachtenberg, F., Stevanovic, S., Ockert, D., Rammensee, H.G., Rieber, E.P., 2000. Generation of survivin-specific CD8+ T effector cells by dendritic cells pulsed with protein or selected peptides. Cancer Res. 60, 4845–4849.

Schulz, O., Diebold, S.S., Chen, M., Näslund, T.I., Nolte, M.A., Alexopoulou, L., Azuma, Y.T., Flavell, R.A., Liljeström, P., Reis e Sousa, C., 2005. Toll-like receptor 3 promotes cross-priming to virus-infected cells. Nature 433, 887–892.

Seya, T., Matsumoto, M., 2009. The extrinsic RNA-sensing pathway for adjuvant immunotherapy of cancer. Cancer Immunol. Immunother. 58, 1175–1184.

Seya, T., Azuma, M., Matsumoto, M., 2013. Targeting TLR3 with no RIG-I/MDA5 activation is effective in immunotherapy for cancer. Expert Opin. Ther. Targets 17, 533–544.

Shime, H., Matsumoto, M., Oshiumi, H., Tanaka, S., Nakane, A., Iwakura, Y., Tahara, H., Inoue, N., Seya, T., 2012. Toll-like receptor 3 signaling converts tumor-supporting myeloid cells to tumoricidal effectors. Proc. Natl. Acad. Sci. U. S. A. 109, 2066–2071.

Topalian, S.L., Gonzales, M.I., Parkhurst, M., Li, Y.F., Southwood, S., Sette, A., Rosenberg, S.A., Robbins, P.F., 1996. Melanoma-specific CD4+ T cells recognize nonmutated HLA-DR-restricted tyrosinase epitopes. J. Exp. Med. 183, 1965–1971.

Tsuruma, T., Iwayama, Y., Ohmura, T., Katsuramaki, T., Hata, F., Furuhata, T., Yamaguchi, K., Kimura, Y., Torigoe, T., Toyota, N., Yagihashi, A., Hirohashi, Y., Asanuma, H., Shimozawa, K., Okazaki, M., Mizushima, Y., Nomura, N., Sato, N., Hirata, K., 2008. Clinical and immunological evaluation of anti-apoptosis protein, survivin-derived peptide vaccine in phase I clinical study for patients with advanced or recurrent breast cancer. J. Transl. Med. 6, 24.

Yamazaki, S., Okada, K., Maruyama, A., Matsumoto, M., Yagita, H., Seya, T., 2011. TLR2-dependent induction of IL-10 and Foxp3+ CD25+ CD4+ regulatory T cells prevents effective anti-tumor immunity induced by Pam2 lipopeptides in vivo. PLOS ONE 6, e18833.

Cancer-Associated Oxidase ERO1-α Regulates the Expression of MHC Class I Molecule via Oxidative Folding

Kazuharu Kukita,*,† Yasuaki Tamura,* Tsutomu Tanaka,* Toshimitsu Kajiwara,* Goro Kutomi,† Keita Saito,† Koichi Okuya,† Akari Takaya,* Takayuki Kanaseki,* Tomohide Tsukahara,* Yoshihiko Hirohashi,* Toshihiko Torigoe,* Tomohisa Furuhata,† Koichi Hirata,† and Noriyuki Sato*

ERO1-α is an oxidizing enzyme that exists in the endoplasmic reticulum and is induced under hypoxia. It reoxidizes the reduced form of protein disulfide isomerase that has oxidized target proteins. We found that ERO1-α is overexpressed in a variety of tumor types. MHC class I H chain (HC) has two disulfide bonds in the α2 and α3 domains. MHC class I HC folding is linked to the assembly of MHC class I molecules because only fully disulfide-bonded class I HCs efficiently assemble with β_2-microglobulin. In this study, we show that ERO1-α associates with protein disulfide isomerase, calnexin, and immature MHC class I before being incorporated into the TAP-1–associated peptide-loading complex. Importantly, ERO1-α regulates the redox state as well as cell surface expression of MHC class I, leading to alteration of susceptibility by $CD8^+$ T cells. Similarly, the ERO1-α expression within cancer cells was associated with the expression level of MHC class I in colon cancer tissues. Thus, the cancer-associated ERO1-α regulates the expression of the MHC class I molecule via oxidative folding *The Journal of Immunology*, **2015, 194: 4988–4996.**

As is widely known, a low-oxygen environment essentially presents in a solid tumor. Therefore, to improve the effect of cancer vaccine, it is very important to know how the immune surveillance mechanism is controlled in such a low-oxygen environment. However, it has been unclear whether tumor cells exposed to hypoxia properly present tumor Ag in the context of MHC class I molecules to $CD8^+$ T cells. The mature MHC class I is composed of H chain (HC), β_2-microglobulin (β2m), and antigenic peptide. Early events in MHC class I assembly involve interactions between MHC class I HC and calnexin, the oxidoreductase ERp57, and β2m (1, 2). Calnexin binds to newly synthesized free HC via a lectin interaction, facilitates the folding of MHC class I HC, and prevents aggregation. MHC class I HC has two disulfide bonds in the α2 and α3 domains. One disulfide bond (Cys^{203}–Cys^{259}) is formed in the hydrophobic core of the α3 domain of MHC class I molecules. The other disulfide bond (Cys^{101}–Cys^{164}) is part of the α1–α2 peptide-binding domain that remains incompletely folded as long as the binding groove is not stably occupied by a peptide (3). Fully oxidized HCs dissociate from calnexin and associate with β2m to form the heterodimeric MHC class I peptide receptor, leading to the association with multiple endoplasmic reticulum (ER)-resident proteins, including TAP, transmembrane glycoprotein tapasin, the chaperone calreticulin, and ERp57 (3). These proteins together constitute the MHC class I peptide-loading complex (PLC), a group of chaperones dedicated to the promotion of loading peptides into the binding groove. The PLC retains and stabilizes empty MHC class I molecules until a suitable peptide ligand is bound. Thus, disulfide bond formation within MHC HC is prerequisite for the stable expression of MHC class I. However, until recently, the precise mechanism for this step had not been demonstrated. Recently, Park and colleagues (4, 5) have demonstrated that protein disulfide isomerase (PDI)–mediated redox regulation plays a very important role in the oxidative folding as well as optimal peptide selection of MHC class I molecules through disulfide bond formation. Protein disulfide bond formation in the ER of eukaryotic cells requires two essential proteins, ERO1-α and PDI (6). ERO1-α is a conserved glycoprotein that is associated with the ER membrane and introduces oxidizing equivalents necessary for protein disulfide bond formation into the ER lumen (7, 8). PDI serves as a principal catalyst of thiol–disulfide exchange in the lumen of the ER. Disulfide transfer to the substrate protein by PDI will result in reduction of active sites of PDI, which must be reoxidized to carry out further oxidation. It has been shown that ERO1-α reoxidized reduced PDI (9). Recently, we showed that ERO1-α was overexpressed in a variety of tumor types, and its expression is further augmented under hypoxic conditions (10), suggesting that cancer-associated ERO1-α might play a role in the oxidative folding of MHC class I molecules in association with PDI in tumor cells and, more importantly, in tumor cells under hypoxia. However, the role of ERO1-α in the oxidative folding of MHC class I molecules has not been clarified. In this study, we show that ERO1-α does indeed participate in the oxidative folding of HCs of MHC class I molecules in tumor cells. ERO1-α facilitates oxidative folding of MHC class I molecules in the early stage of folding and assembly of MHC class I through

*Department of Pathology, Sapporo Medical University School of Medicine, Sapporo 060-8556, Japan; and †Department of Surgery, Sapporo Medical University School of Medicine, Sapporo 060-8556, Japan

ORCID: 0000-0002-0112-8730 (Y.T.).

Received for publication December 3, 2013. Accepted for publication February 23, 2015.

This work was supported in part by a Grant-in-Aid for Scientific Research from the Ministry of Education, Culture, Sports, Science and Technology of Japan.

Address correspondence and reprint requests to Dr. Yasuaki Tamura, Department of Pathology, Sapporo Medical University School of Medicine, South 1, West 17, Chuo-ku, Sapporo 060-8556, Japan. E-mail address: ytamura3566@gmail.com

The online version of this article contains supplemental material.

Abbreviations used in this article: BN-PAGE, blue native–PAGE; ER, endoplasmic reticulum; HC, H chain; β2m, β_2-microglobulin; MMTS, methyl methanethiosulfonate; PDI, protein disulfide isomerase; PLC, peptide-loading complex; PRDX IV, peroxiredoxin IV; QSOX, quiescin sulfyhdryl oxidase; shRNA, short hairpin RNA; VKOR, vitamin K epoxide oxidoreductase.

www.jimmunol.org/cgi/doi/10.4049/jimmunol.1303228

PDI reoxidation. In particular, hypoxia-induced ERO1-α plays a profound impact on the oxidative folding and expression of MHC class I molecules.

Materials and Methods

Cell lines and cell culture

The colon cancer cell line SW480 (HLA-A*0201/2402) was cultured in DMEM (Sigma-Aldrich, St. Louis, MO) supplemented with 10% FBS (Invitrogen Life Technologies, Carlsbad, CA). SW480-ERO1-α, a stable transfectant of SW480 cells with ERO1-α cDNA, and SW480–short hairpin RNA (shRNA) ERO1-α, a stable knockdown cell line of SW480 cells with short hairpin RNA for ERO1-α, were cultured in DMEM supplemented with 10% FBS and 4 μg/ml puromycin (Sigma-Aldrich). The human cancer cell lines MCF-7, MIAPaCa2, HCT15, HCT116, and HT29 were purchased from American Type Culture Collection. For preparing hypoxia samples, cells were incubated in 1% O_2 for indicated periods.

Abs

The mouse mAb against ERO1-α was purchased from Abnova, and a rabbit polyclonal Ab to ERO1-α was purchased from Novus. Anti β-actin was from Sigma-Aldrich. The mouse mAb W6/32, which binds a conformational epitope carried by all HLA-A, -B, and -C HCs with β2m and mAb against transferrin receptor (CD71) were purchased from Abcam. Anti-HLA-A, -B, and -C mouse mAb EMR8.5, which recognizes both folded and unfolded MHC class I HCs, was purchased from Hokudo (Sapporo, Japan). Anti-HLA-A, -B, and -C mouse mAb HC-10, which recognizes unfolded MHC class I HCs, was purchased from Nordic-MUbio (Susteren, the Netherlands). Rabbit polyclonal Ab PDI, calnexin, and ERp57 were purchased from Enzo Life Sciences. The mouse mAb 148.3 directed against the C terminus of human TAP1 was a gift from Dr. Cresswell (Yale University). Anti-β2m rabbit polyclonal Ab was purchased from Dako-Cytomation. Anti-β2m mouse mAb BBM1, goat polyclonal Ab against peroxiredoxin IV (PRDX IV), quiescin sulfhydryl oxidase (QSOX), and rabbit polyclonal Ab aginst vitamin K epoxide oxidoreductase (VKOR) were purchased from Santa Cruz Biotechnology.

Constructs

A myc-tagged human ERO1-α cDNA construct was generated by PCR and inserted into the NheI-XhoI site of the pIRESpuroIII vector (Invitrogen Life Technologies). A c-myc tag was added to the C-terminal end of ERO1-α. Four unique 29-mer shRNA constructs against ERO1-α in the pRS vector and control shRNA vector were purchased from OriGene (Rockville, MD). Western blotting showed that only one of four shRNA constructs was effective to deplete ERO1-α in SW480 cells. Therefore, we established three stable clones of ERO1-α–depleted cells and confirmed that they showed quite similar results in the MHC class I assembly.

Western blotting

Normal colon tissue extract was purchased from Santa Cruz Biotechnology (Dallas, TX). For blockade of free thiols, cells were pretreated for 5 min with 10 mM methyl methanethiosulfonate (MMTS; Pierce, Rockford, IL). Cells were lysed in 1% Nonidet P-40 in TBS buffer containing 25 mM HEPES, 100 mM NaCl, 10 mM $CaCl_2$, and 5 mM $MgCl_2$ (pH 7.6) supplemented with a protease inhibitor and 5 mM MMTS. Postnuclear supernatants were divided and heated for 5 min at 95°C in nonreducing or reducing SDS sample buffer, resolved by 10% SDS-PAGE, and electrophoretically transferred to polyvinylidene difluoride membranes (Immobilon-P; Millipore, Billerica, MA). The membranes were incubated with blocking buffer (5% nonfat dry milk in PBS), probed with primary and secondary Abs, and proteins were visualized using ECL detection system (Amersham Life Science, Arlington Heights, IL).

Immunoprecipitation

Cells were lysed in 1% digitonin in TBS (50 mM Tris-HCl, 150 mM NaCl [pH 8.0]) supplemented with protease inhibitor. Postnuclear supernatant was precleared for 2 h with 3 μl normal mouse serum and 30 μl (50% slurry) protein G–Sepharose beads (Amersham Pharmacia, Piscataway, NJ) and then incubated with 3 μg appropriate Ab and 50 μl protein G–Sepharose beads (50% slurry) for 4 h. After precipitation, beads were washed five times with 1% Triton X-100 in TBS. Precipitated proteins were eluted by boiling in Laemmli buffer and analyzed by Western blotting.

Real-time RT-PCR

Multiple tissue cDNA panels were purchased from Clontech (Palo Alto, CA). Total RNA was isolated from cultured cells by using Isogen reagent (Nippon Gene, Tokyo, Japan). The cDNA mixture was synthesized from 1 μg total RNA by reverse transcription using SuperScript III and oligonucleotide (deoxythymidine) primer (Invitrogen Life Technologies, Gaithersburg, MD). Real-time PCR was performed to determine the expression levels of ERO1-α and β-actin. Expression values for each sample were normalized to β-actin, and fold levels of the indicated genes represent the mean (±SEM) of replicate reactions. Primer sequences were as follows: β-actin (ACTB), Hs0160665_g1; ERO1-α (ERO1L), Hs00205880_m1; and HLA-A, Hs01058806_g1 (Life Technologies). PCR cycles were performed on the StepOne real-time PCR system (Life Technologies) with the following cycle conditions: 10 min at 95°C, 40 cycles of 15 s at 95°C and 1 min at 60°C. The ΔΔCt method was used for data analysis.

Blue native–PAGE

First-dimensional blue native (BN)-PAGE and second-dimensional SDS-PAGE were conducted according to instructions in the user's manual of NativePAGE Novex Bis-Tris gel system (Invitrogen Life Technologies) with only the following modification. For preparation of samples, a total of 1×10^6 cells were lysed in 1 ml 1× NativePAGE sample buffer (50 mM Bis-Tris buffer, 50 mM NaCl, 6 N HCl, 10% glycerol, and 0.0001% Ponceau S [pH 7.2]) containing 1% digitonin.

DTT washout assays

For measuring the recovery of folded MHC class I (oxidized form) after DTT treatment, cells were grown in 6-cm dishes and incubated for 10 min in a medium containing 10 mM DTT at room temperature. The cell monolayers were then quickly washed twice with 2 ml PBS at room temperature and, for oxidative recovery, covered again with DMEM. For the 0 s time point, this incubation step was omitted. The oxidative reaction was stopped by the removal of DMEM and addition of ice-cold PBS with 10 mM MMTS. For visualization of the MHC class I redox states upon DTT washout, nonreducing SDS-PAGE samples were prepared in the manner described above. Samples were analyzed by Western blotting.

Acid strip assay

MHC class I–peptide complexes expressed on cell the surface can be eluted with citrate acid treatment. For measuring the recovery of cell surface expression of MHC class I after acid treatment, cells ($\sim 5 \times 10^5$) were grown in 6-cm dishes and incubated for 2 min in 2 ml citrate phosphate buffer at pH 3.0 (0.131 M citric acid, 0.066 M Na_2HPO_4, 150 mM NaCl) at room temperature. The cell monolayers were then quickly washed twice with 2 ml appropriate medium (pH 7.4) and either reincubated in a fresh medium or prepared for flow cytometry analysis.

Flow cytometric analysis

Cells were incubated with W6/32 or anti-CD71 Ab, coupled with FITC at a saturation concentration for 30 min on ice, and then washed with PBS. Samples were analyzed using a BD FACCalibur flow cytometry system (Becton Dickinson, Mountain View, CA).

IFN-γ assay for T cell response

SW480 cells were cocultured with a survivin (apoptosis-related gene expressed in SW480 cells)-specific CTL clone (11) at an indicated E:T ratio. After 24 h incubation, cocultured supernatants were collected and IFN-γ was measured by ELISA (R&D Systems, Minneapolis, MN).

Immunohistochemistry

Immunohistochemistry was conducted according to Institutional Review Board guidelines for the use of human subjects in research. Formalin-fixed paraffin-embedded sections of surgical specimens from colon cancer patients ($n = 85$) were used in the immunohistochemistry. Reactivity of the anti-HLA-A, -B, and -C mouse mAb EMR8.5 was determined by staining the plasma membranes of tumor cells. Reactivity of the anti–ERO1-α mAb was determined by perinuclear staining within tumor cells, indicating ER localization. The expression status of MHC class I was graded semiquantitatively according to the modified classification as described previously (12): score 1 (positive cells < 20%), score 2 (20% ≤ positive cells ≤ 80%), and score 3 (positive cells > 80%) (see Fig. 8B). Total populations of score 1 and score 2 were included as the MHC I reduced group and score 3 was regarded as the MHC class I–positive group. The expression status of ERO1-α was graded by our original classification: score 0 (positive cells 0%), score 1 (positive cells < 30%), score 2 (30% ≤ positive cells ≤ 80%), score 3

(positive cells > 80%) (see Fig. 8A). In cases where there are apparent dot-like stainings that indicate the abundant expression within ER, the scoring number is one point up. Total populations of scores 0, 1, and 2 were included as the ERO1-α reduced group and score 3 was regarded as the ERO1-α–positive group. The relationship between MHC class I expression and ERO1-α expression on tumor cells was analyzed using a Spearman rank correlation coefficient and odds ratio. A p value <0.05 was considered statistically significant.

Statistical analysis

All experiments except for the immunohistochemistry were independently performed in triplicate. Results are given as means ± SEM. Comparisons between two groups were performed using a Student t test, with a p value <0.05 considered to be statistically significant.

Results

ERO1-α expression in normal tissues and various types of cancer cell lines

Expression of ERO1-α was detected at modest levels in the skeletal muscle, heart, liver, and pancreas by real-time RT-PCR (Fig. 1A). In clear contrast, ERO1-α was expressed at high levels in various types of cancer cell lines, including the human colon cancer cell line SW480, breast cancer cell line MCF-7, and pancreatic cancer cell line MIAPaCa2 (Fig. 1A). To confirm these observations, we examined protein levels of ERO1-α in normal colon tissues and colon cancer cell lines (HCT15, HCT116, HT29, and SW480) by Western blotting. The normal colon tissue did not express ERO1-α protein, whereas all of the cancer cell lines examined expressed ERO1-α protein at high levels as shown by Western blotting (Fig. 1B). In immunohistochemical analysis using an anti–ERO1-α mAb, we observed that normal colon tissues revealed negative staining for ERO1-α (Fig. 1Ci, Supplemental Fig. 1A, 1B). In contrast, perinuclear expression of ERO1-α, indicating ER localization, was found in colon cancer tissues (Fig. 1Cii, iii, Supplemental Fig. 1C–F). We observed a patchy staining pattern of ERO1-α within the cancer nests. It has been demonstrated that hypoxic areas are frequently present within cancer tissues. Because ERO1-α is induced under a hypoxia condition, we assumed that cancer cells residing within hypoxic areas showed augmented expression of ERO1-α. Thus, heterogeneity of ERO1-α expression seems to be attributed to oxygen and blood supply. These results suggested that ERO1-α might play a role as an oxidase within cancer cells and under some specific conditions such as hypoxia, which is frequently observed within cancer tissues. Therefore, we examined whether ERO1-α plays a role in the oxidative folding of MHC class I molecules in cancer cells.

ERO1-α regulates redox status of MHC class I HC via PDI oxidation

To begin, we established a human colon cancer cell line SW480 with ERO1-α overexpression or knockdown. To monitor the

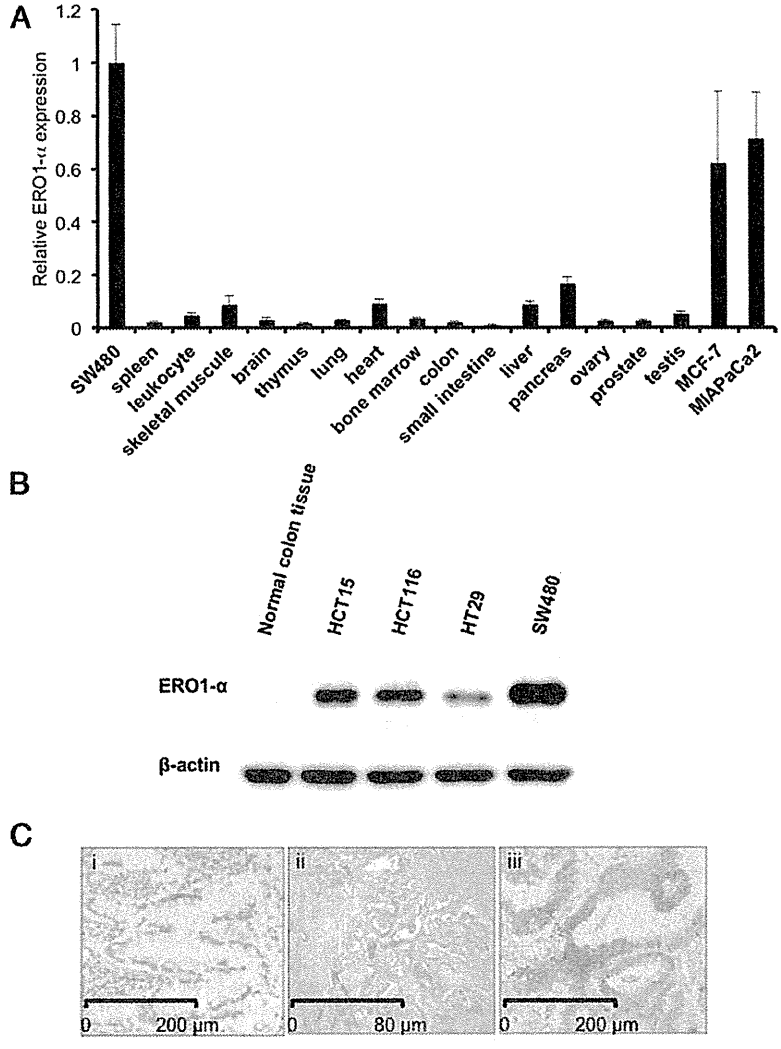

FIGURE 1. Expression of ERO1-α in normal tissues, human cancer cell lines, and cancer tissues. **(A)** Relative ERO1-α mRNA levels in normal tissues and cancer cell lines. Real-time relative PCR (real-time PCR) was performed to determine the expression levels of ERO1-α and β-actin. Expression values for each sample were normalized to β-actin, and fold levels of the indicated genes represent the mean (±SEM) of replicate reactions. Data from one of four independent experiments are depicted. **(B)** Western blot analysis of normal colon tissue and colon cancer cell lines. β-actin was used as a loading control. **(C)** Immunohistochemistry of human normal colon tissue (i) and colon cancer tissue (ii and iii) using anti–ERO1-α mAb. Tissue sections were developed using diaminobenzidine.

disulfide status (oxidized form or reduced form) of ERO1-α, PDI, and MHC class I HC, free thiols were modified with the thiol-alkylating reagent MMTS, and the samples were divided and denatured under a reducing or nonreducing condition so that we could monitor the disulfide status of these proteins by mobility shift. Western blot analysis revealed that the ERO1-α–PDI mixed disulfides migrated with an apparent molecular mass of ~140 kDa under a nonreducing condition (Fig. 2A). Interestingly, in cells with ERO1-α overexpression, almost all of the PDI formed a complex with ERO1-α by a disulfide bond link. Moreover, the oxidized form of MHC class I HC was increased compared with that in WT cells. Knockdown of ERO1-α in SW480 cells decreased the complex of ERO1-α–PDI formed by mixed disulfide bond formation, indicating that depletion of ERO1-α decreased the oxidized form of PDI (Fig. 2B). At the same time, the total amount of MHC class I HC was decreased under a reducing condition, and both oxidized and reduced forms of MHC class I HC were also decreased under a nonreducing condition. These findings suggested that depletion of ERO1-α decreased disulfide bond formation in MHC class I HC, making it an unfolded protein, resulting in the degradation of unfolded MHC class I HC. Thus, ERO1-α clearly affects the redox status of PDI and oxidative folding of MHC class I HC.

ERO1-α regulates the oxidative folding of MHC class I HC

To assess the impact of ERO1-α on the disulfide bond formation of MHC class I HC, we used a DTT washout assay. Cells were treated with 10 mM DTT to retain the reduced form of MHC class I HC until the initiation of the chase. In our assay, ~50% of total MHC class I HCs were oxidized after 15 min chase in SW480 cells. We observed that appearance of oxidized MHC class I HCs was faster in cells with ERO1-α overexpression than in WT or ERO1-α knockdown cells (Fig. 3A, 3B). Oxidation of MHC class I HCs was observed after 3 min chase in ERO1-α–overexpressed cells. In contrast, MHC class I HC remained as the reduced form after 3 min chase in ERO1-α knockdown cells. To kinetically assess the impact of ERO1-α on peptide loading, we examined the acid strip assay. Cells were acid washed to denature surface MHC class I–β2m dimers, and the rate of arrival of new molecules at the cell surface was monitored by flow cytometry (Fig. 3C). Total MHC class I recovery and rate of recovery were highest in cells with ERO1-α overexpression. Thus, the expression of ERO1-α is likely to reflect the assembly efficiency of MHC class I molecules in combination with their stability at the cell surface, which generally correlates with the quality of the associated peptide repertoire. This may be due to the fact that ERO1-α increases oxidized PDI, resulting in efficient optimal peptide selection by PDI, as demonstrated by Park et al. (4).

ERO1-α activity in MHC class I Ag presentation

To investigate the function of ERO1-α in MHC class I expression, we used cells with transfected ERO1-α and RNA interference for knockdown of endogenous ERO1-α. As detected with the conformation-specific mAb W6/32, surface expression of fully folded class I molecules was augmented up to 2.5-fold in ERO1-α–overexpressing SW480 cells compared with that in WT cells (Fig. 4A, 4E). In contrast, surface level of class I molecules was reduced to 60% in ERO1-α knockdown cells compared with that in WT cells (Fig. 4B, 4F). Unexpectedly, depletion of ERO1-α did not affect the surface expression of disulfide-bonded glycoprotein CD71, suggesting that the ERO1-α–PDI pathway is not essential for the maturation of CD71 glycoproteins in these cells (Fig. 4C, 4D, 4G, and 4H).

Role of ERO1-α in CTL recognition

Effectiveness of the Ag processing machinery is ideally assessed by sensitivity to CTL. We used HLA-A*2402–restricted T cell clones recognizing peptides derived from the cancer Ag survivin 2B. SW480 cells with ERO1-α overexpression or depletion were

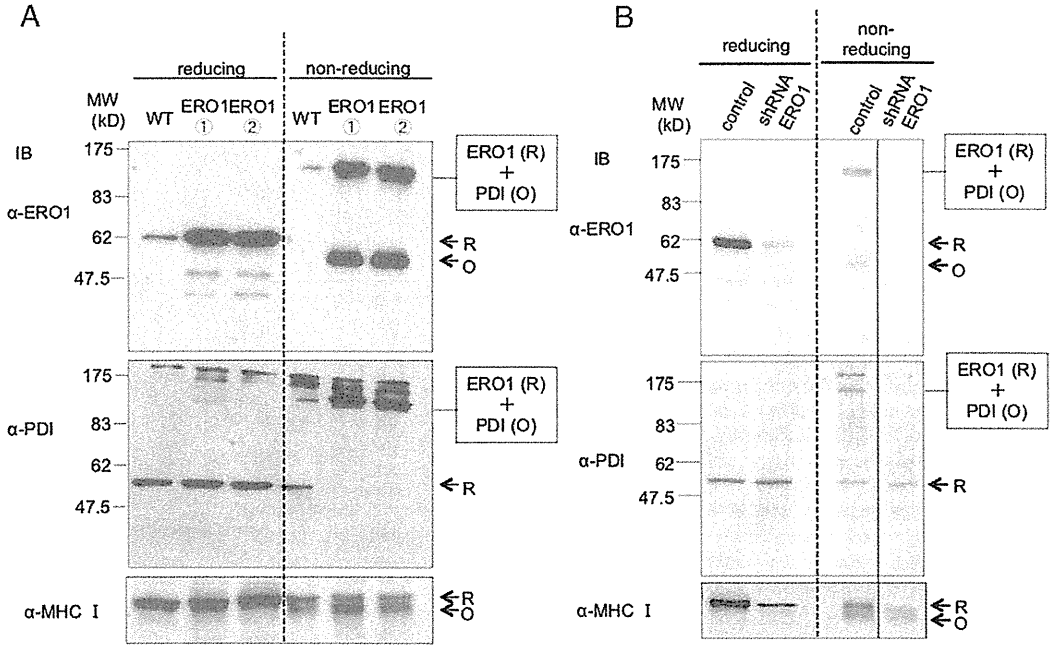

FIGURE 2. Formation by ERO1-α of a mixed disulfide linkage with PDI and effects of ERO1-α overexpression and depletion on the redox status of MHC class I HC. (**A**) Redox status of ERO1-α, PDI, and MHC class I HC in SW480 cells, cells with ERO1-α overexpression. Reduced form (R) and oxidized form (O) of ERO1-α, PDI, or MHC class I HC are indicated. Note that overexpression of ERO1-α increased ERO1-α–PDI complex as well as oxidized MHC class I HC. (**B**) ERO1-α–depleted cells were examined by Western blotting under reducing or nonreducing conditions. Depletion of ERO1-α decreased the ERO1-α–PDI complex and both oxidized and reduced forms of MHC class I HC. The black line indicates where parts of the image were joined.

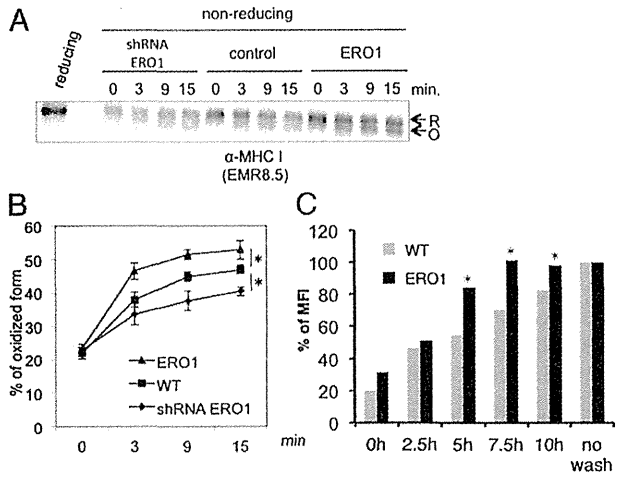

FIGURE 3. ERO1-α regulates the oxidative folding of MHC class I HC. **(A)** Recovery of folded MHC class I HC in SW480 WT cells and SW480 cells with ERO1-α overexpression or knockdown after DTT treatment. Cells were treated with 10 mM DTT and chased for 0, 3, 9, and 15 min. Nonreducing SDS-PAGE samples were prepared and immunoblotted with anti–MHC class I mAb. **(B)** Plots show the percentage oxidized form (O) of all MHC class I (reduced form [R] and oxidized form). **(C)** The impact of ERO1-α on peptide loading onto MHC class I molecules. Cells were acid washed using citrate phosphate buffer (pH 3.0) to denature surface MHC class I–β2m dimers and the rate of arrival of new molecules at the cell surface was monitored by flow cytometry. Relative MHC class I cell surface expression was plotted as percentage of mean fluorescence intensity (MFI) after acid strip. $*p < 0.05$.

tested for recognition by the survivin 2B–specific CTL using an IFN-γ production assay. IFN-γ production was apparently augmented when cells with ERO1-α overexpression were used as target cells (Fig. 4I). In clear contrast, ERO1-α depletion inhibited CTL activity. Thus, these findings indicated that ERO1-α plays a pivotal role in MHC class I Ag presentation.

ERO1-α forms a complex with PDI, calnexin, and unfolded MHC class I HC

We next examined at which stage ERO1-α is involved in MHC class I assembly. To study the ERO1-α–involved process of MHC class I assembly, we used an immunoprecipitation assay, followed by Western blotting. We observed that ERO1-α associated with MHC class I HC detected by EMR8.5 (recognized both unfolded MHC class I HC and folded MHC class I HC) and HC-10 (recognized unfolded MHC class I HC), PDI, and calnexin but not with MHC class I detected by W6/32 mAb that recognizes the folded MHC class I–β2m heterodimer, or mAb against β2m (Fig. 5A). Likewise, immunoprecipitates made with mAb W6/32 did not include ERO1-α, suggesting that folded MHC class I did not interact with ERO1-α. Most importantly, TAP1 and ERO1-α were not coimmunoprecipitated with each other, indicating that ERO1-α is not a member of TAP-associated MHC class I PLC (Fig. 5B). As shown in Fig. 2, Western blotting analysis under nonreducing condition indicated that ERO1-α was exclusively associated with PDI via a disulfide bond link. In contrast, results from immunoprecipitation experiments suggested that ERO1-α associated with unfolded MHC class I HC and calnexin via a non–covalent bond. As Park et al. (4) have demonstrated that PDI bound unfolded MHC class I HC via disulfide bond, these findings indicated that ERO1-α bound to PDI to reoxidize it, and then oxidized PDI forms a disulfide bond within unfolded MHC class I HC before reaching the TAP-associated PLC stage. From the standpoint of electron transfer, we assumed that electron flow from MHC class I HC to oxidized PDI and subsequently to ERO1-α is a relay line for the ERO1-α–PDI oxidative folding pathway.

Molecular architecture of ERO1-α–associated MHC class I molecules

BN-PAGE has been used to analyze the molecular composition of various multisubunit complexes, including B and T cell Ag receptors and TAP-associated MHC class I PLC (13). Therefore,

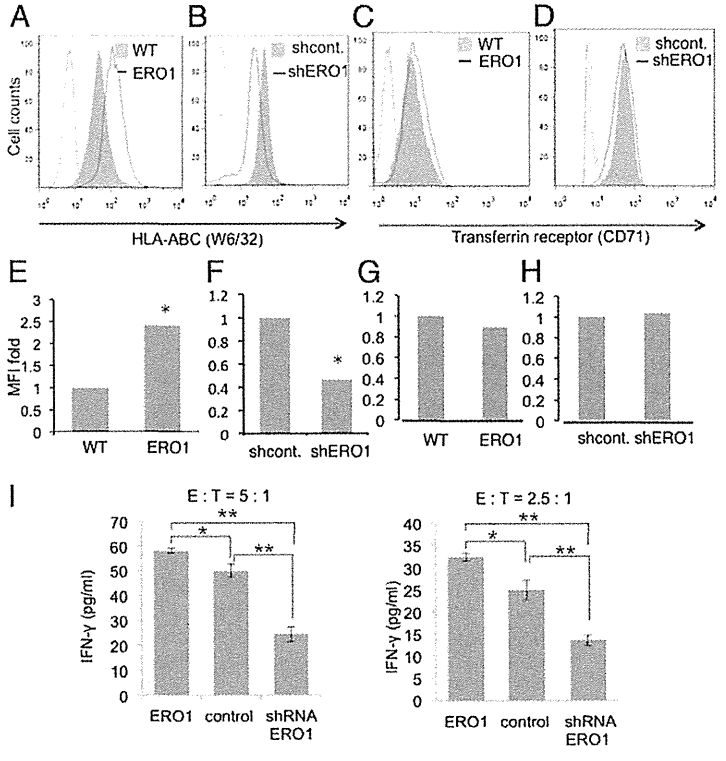

FIGURE 4. ERO1-α regulates cytotoxic T cell responses. **(A–H)** Effect of ERO1-α on cell surface expression of MHC class I molecules. SW480 cells with ERO1-α overexpression (A and E) or depletion (B and F) were analyzed for surface levels of MHC class I molecules. The expression of transferrin receptor (CD71) was also compared (C, D, G, and H). Control Ab staining, thin line and dotted line. The mean fluorescence intensity (MFI) value obtained in WT SW480 cells or shRNA control cells was set as 1, and the differences in MFI induced by ERO1-α overexpression and knockdown were plotted. **(I)** Ag presentation is impaired in cells with depletion of ERO1-α. Survivin 2B–specific CTLs were cocultured with SW480 cells or SW480 cells with ERO1-α overexpression or depletion at a ratio of 5:1 or 2.5:1. IFN-γ in the culture supernatant was measured using ELISA. Data from one of four independent experiments are depicted. Mean values of triplicate are shown (±SD). $*p < 0.05$, $**p < 0.01$.